Chapter 3

Results and Discussion

3. Results and discussion:

The work done has been divided into four parts which have been presented in four major sections in this chapter.

3.1. Utilization of coexisting iron for simultaneous removal of removal of As and Fe by OCOP*:

In this work, coexisting iron ($[Fe^{2+}]_o$) was utilized for removal of arsenic from groundwater sources as coagulant in lieu or with minimum addition of coagulant $FeCl_3$ in the OCOP method [30]. Results of the batch experiment for utilization of the coexisting iron along with optimization of the doses of pH conditioner ($NaHCO_3$) and oxidant ($KMnO_4$) by RSM with respect to $[Fe^{2+}]_o$ are analysed in this section [30]. Here we our intention was to lower the cost of the OCOP process by utilizing coexisting iron instead of externally added full dose of $FeCl_3$ of the OCOP and to increase the removal efficiency of arsenic compared to the OCOP method by optimizing the doses [30]. We have also verified the experimental results with a field trial conducted in some selected arsenic contaminated areas of Assam, India.
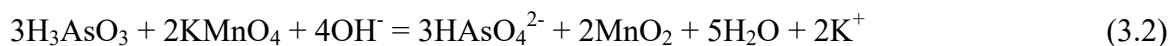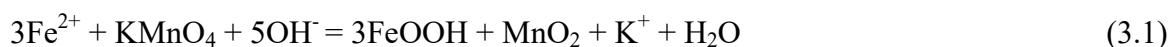
3.1.1. Batch experiment:

The experimental procedure involves a series of oxidation-coagulation-adsorption experiment (OCOP) was performed in five 1 L beakers containing tap water with a fixed initial As^{3+} concentration of 100 µg/L and initial concentration of ferrous iron (i.e., $[Fe^{2+}]_0$) varied as 5, 10, 15, 20, and 25 mg/L, respectively, taken as the coexisting iron. Here 2 or 3 drop of pH conditioner 9% $NaHCO_3$ solution was added first to each beaker to increase the pH to about 8-9. Because at higher pH oxidation of As^{3+} by $KMnO_4$ is found to better and removal efficiencies of arsenic by coexisting iron was reported as good with increase in pH of the water [216]. Then, $KMnO_4$ solution was added to get varying $KMnO_4$ concentrations from 5% to 100% equivalent of $[Fe^{2+}]_0$ with an interval of 5%. Thirdly aqueous $FeCl_3$ solution was added as equal to the difference between the coagulant dose (25 mg/L) of the OCOP method and the coexisting iron concentration, i.e., as (25 mg/L‑$[Fe^{2+}]_0$). As $FeCl_3$ lowers the pH, more $NaHCO_3$ is then added drop wise to adjust the final pH in the range of 7.0–7.3, a favourable range for arsenic removal.

3.1.2. Observations with Explanations:

From the results of batch experiment, plots of remaining concentration of arsenic *vs.* $KMnO_4$ dose in percentage equivalent of $[Fe^{2+}]_o$ for different $[Fe^{2+}]_o$ was prepared and represented in the **Figure 3.1** [30]. Removal of arsenic was found to be increased with increase in $[Fe^{2+}]_o$ and $KMnO_4$ dose. The increased removal efficiency of arsenic with increase in the $KMnO_4$ dose is genuine because it oxidizes As^{3+} ions to easily removable As^{5+} ions and can be easily attributed to a contribution to coagulation by the newly formed Fe^{3+} ions, from oxidation of Fe^{2+} ions [218]. The arsenic removal with increase in coexisting iron concentration, $[Fe^{2+}]_o$ may be ascribed to increase in the coagulation as well as to increasing formation of MnO_2. Since we added the $KMnO_4$ dose is in percent equivalent of $[Fe^{2+}]_o$, the net amount of $KMnO_4$ in mol increases with $[Fe^{2+}]_o$ resulting more formation of MnO_2. MnO_2 is formed due to the reaction between $[Fe^{2+}]_o$ and $KMnO_4$ in the aqueous alkaline medium in presence of $NaHCO_3$. The precipitated solid MnO_2 helps in arsenic removal by adsorbing arsenate, As^{5+} ions [78, 97].

The reactions can be summarised as [218, 263]:

$$3Fe^{2+} + KMnO_4 + 5OH^- = 3FeOOH + MnO_2 + K^+ + H_2O \qquad (3.1)$$

$$3H_3AsO_3 + 2KMnO_4 + 4OH^- = 3HAsO_4^{2-} + 2MnO_2 + 5H_2O + 2K^+ \qquad (3.2)$$

Therefore, the observed arsenic removal to below 2 µg/L at comparatively lower concentration of $FeCl_3$ (25 mg/L) can rightly be accepted due to adsorption of arsenate ions, As^{5+} on MnO_2 precipitates in addition to the adsorption on the coagulates formed by $FeCl_3$.

Figure 3.1 also shows that required dose of $KMnO_4$ is about 80% to 95% equivalent of $[Fe^{2+}]_o$ for removal of arsenic to less than 2 µg/L indicating the $KMnO_4$ dose required to oxidise all the coexisting ferrous ions and arsenite ions. It was reported that at prevailing pH of about 7.0-7.3 controlled by $NaHCO_3$, the $FeCl_3$ forms coagulates consisting of predominantly amorphous goethite (FeOOH) and some amount of iron oxides such as Fe_2O_3 and $Fe(OH)_3$ which adsorbs arsenate ions, As^{5+} present in the anionic forms: $H_2AsO_4^-$ and $HAsO_4^{2-}$ [218].

It is interesting to note that at the beginning removal efficiencies of arsenic increases rapidly on increasing the $KMnO_4$ dose and after that slows down above a $KMnO_4$ dose of about 15% equivalent of $[Fe^{2+}]_o$ and again increases rapidly above a $KMnO_4$ dose about 50%

equivalent of $[Fe^{2+}]_o$. This can be explained with the fact that the oxidation of arsenite to arsenate and reduction of arsenate to arsenite are rather slow processes [78, 202]. The presence of the redox couple, $Fe^{2+} \leftrightarrow Fe^{3+}$ and variations of the reduction potentials with pH further complicate the $As^{3+} \leftrightarrow As^{5+}$ redox equilibrium [264]. As a result, some As^{3+} ions exist even in oxidising situations and similarly some of As^{5+} ions also exist even in reducing situations [78]. So the observed initial rapid arsenic removal on addition of $KMnO_4$ in lower percentage (5-15%) equivalent of $[Fe^{2+}]_o$ may be attributed to a rapid adsorption of the already existing As^{5+} ions on the coagulates formed by externally added Fe^{3+} ions and by a rapid oxidation of Fe^{2+} by $KMnO_4$. It is evocative to mention here that the negatively charged arsenate forms of arsenic, viz., $H_2AsO_4^-$ and $HAsO_4^{2-}$, are easily adsorbed compared to the mostly uncharged arsenite (H_3AsO_3) form by the coagulates at the prevailing pH of about 7.3 in the presence of $NaHCO_3$ [95, 264, 265]. At the experimental pH range, the $Fe^{2+} \leftrightarrow Fe^{3+}$ redox couple has a lower reduction potential than that of the $As^{3+} \leftrightarrow As^{5+}$ and hence Fe^{2+} ions are preferentially oxidised over As^{3+} by $KMnO_4$ [264].

With high concentration of coexisting Fe^{2+} ions, [264] [78] the added $KMnO_4$ dose was consumed by coexisting Fe^{2+} ions before oxidation of As^{3+} in the intermediate range of $KMnO_4$ dose [218]. Therefore, the arsenic removal increases slowly in intermediate range due to poor adsorption of the As^{3+} ions despite an increase in the coagulation due to formation of more Fe^{3+} ions arising from the oxidation of coexisting, Fe^{2+}. Oxidation of As^{3+} to As^{5+} ions occurs at higher $KMnO_4$ dose and therefore are easily adsorbed by coagulates resulting in a rapid arsenic removal as shown in **Figure 3.1**. The minimum required doses of oxidant, $KMnO_4$ and pH conditioner, $NaHCO_3$ for arsenic removal from 100 µg/L to less than 2 µg/L in presence of coexisting iron concentration, $[Fe^{2+}]_0$ of 5, 10, 15, 20, and 25 mg/L were assessed from the experimental results shown in **Figure 3.1** are represented by **Figure 3.2**.

From the batch experiment we predicted the required doses of $KMnO_4$, in equivalent percentage of $[Fe^{2+}]_o$, for the entire range of $[Fe^{2+}]_o$ for practical applications as: 95%, 93%, 90%, 85%, and 80% for $[Fe^{2+}]_o$ in the ranges of 0–5, >5–10, >10–15, >15–20, and >20–25 mg/L, respectively. The gradual decrease in the minimum required $KMnO_4$ dose with increase in $[Fe^{2+}]_o$ may be attributed to an increasing adsorption of arsenic by MnO_2 as the precipitation of the later increases with increase in $[Fe^{2+}]_o$ [97].
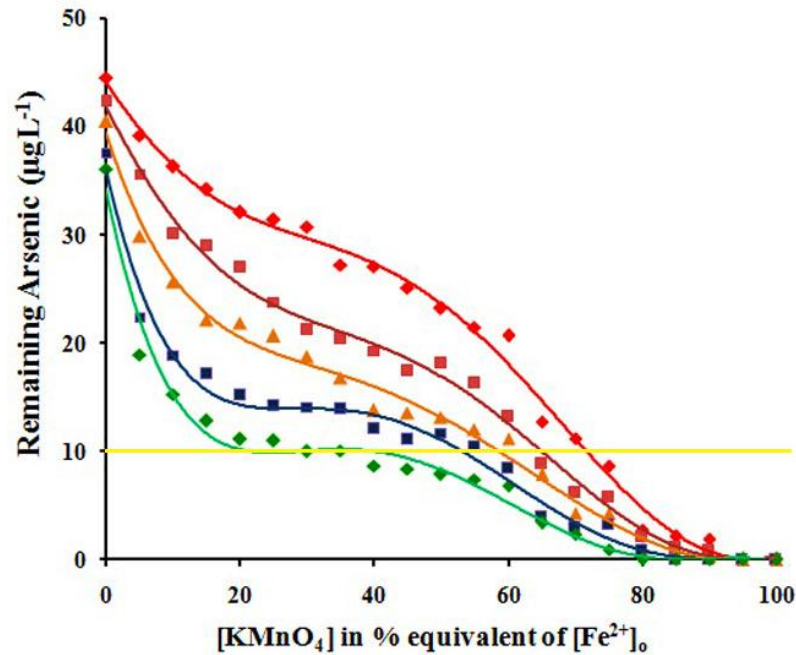
Figure 3.1: Plots of remaining concentration of arsenic *vs*. $KMnO_4$ dose in percentage equivalent of $[Fe^{2+}]_o$ for different $[Fe^{2+}]_o$. The dose of $FeCl_3$ = (25 mg/L – $[Fe^{2+}]_o$). Symbols: ♦ - 5 mg/L Fe^{2+}, ■ -10 mg/L Fe^{2+}, ▲ -15 mg/L Fe^{2+}, ■ - 20 mg/L Fe^{2+}, ♦ - 25 mg/L Fe^{2+}. The horizontal yellow line indicates the WHO guideline value.

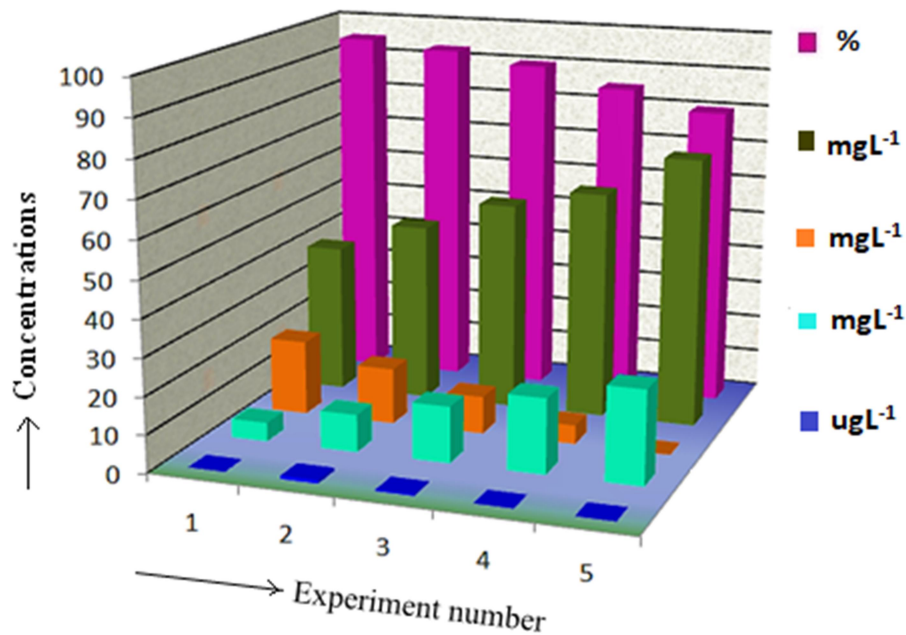**Figure 3.2:** The doses of $NaHCO_3$ and $FeCl_3$, and the minimum dose of $KMnO_4$, in percentage equivalent of $[Fe^{2+}]_o$, required for removal of arsenic from 100 μg/L to < 2 μg/L at different initial ferrous iron concentrations ($[Fe^{2+}]_o$). Symbols: ■ - Remaining As, ■ - Initial iron, Fe^{2+}, ■ - $FeCl_3$, ■ - $NaHCO_3$, and ■ - $KMnO_4$ (In % equivalent of $[Fe^{2+}]_o$).

3.1.3. Optimization of the doses by RSM:

3.1.3.1. Experimental design:

The batch experimental data presented in **Figure 3.1** were analysed by RSM using CCD design and quadratic model to optimize the doses for removal of arsenic from groundwater to less than 2 μg/L. The analysis was performed for the data of the laboratory batch experiments with [KMnO₄] dose of 80%, 85%, 90%, 93% and 95% equivalent of coexisting iron concentration, $[Fe^{2+}]_o$, because in the laboratory experiment arsenic removal was found better in these range of % of KMnO₄. The experimental designs involved the two independent parameters (A and B), each at two levels coded -1 and +1 for low and high concentrations/values, respectively. The coded levels -1 and +1, chosen on the basis of the results in **Figure 3.1** are shown in **Table 3.1**. The experimental data points used in the CCD, with remaining arsenic concentration as response, have been calculated for different KMnO₄ doses presented in **Table 3.2-3.5**.

The coefficients of the response function (main polynomial equation, **Equation 2.3**) for remaining arsenic concentration were obtained using experimental data which can be seen in **Table 3.6**. Three types of 3D plots for each % of KMnO₄ dose (80 %, 85%, 90% and 93%) with remaining arsenic as response in each case and by selecting two independent variables among the three operating variables *viz.* dose of KMnO₄ in % equivalent of $[Fe^{2+}]_o$, dose of NaHCO₃ in mg/L and coexisting iron concentration, $[Fe^{2+}]_o$ in mg/L. So as a whole total twelve 3D plot were prepared as shown in **Figure 3.3**.

The experimental data points used for optimising the KMnO₄ doses, i.e., when the KMnO₄ doses were taken as response are shown in **Table 3.7**. The experimental data points used for optimising the NaHCO₃ doses are also included in **Table 3.7**. **Figure 3.4** shows the 3D plot for optimization of doses of KMnO₄ in percentage equivalent of $[Fe^{2+}]_o$ with variation of $[Fe^{2+}]_o$ and [NaHCO₃]. **Figure 3.4** also includes the 3D plot for optimization of doses of [NaHCO₃] with variation of $[Fe^{2+}]_o$ and [KMnO₄].

Table 3.1: Levels of the factors for central composite design with (a) remaining arsenic as response and (b) with percentage of $KMnO_4$ as response, (c) with $[NaHCO_3]$ as response:

(a) Remaining arsenic as response			
Set of experiment	**Independent factors**	**Coded levels in mg/L**	
		−1	+1
All	$[Fe^{2+}]_o$	5	25
80% equivalent of $[Fe^{2+}]_o$	$[KMnO_4]$	3.77	18.85
	$[NaHCO_3]$	46	72
85% equivalent of $[Fe^{2+}]_o$	$[KMnO_4]$	4.00	20.00
	$[NaHCO_3]$	45	70
90% equivalent of $[Fe^{2+}]_o$	$[KMnO_4]$	4.20	21.00
	$[NaHCO_3]$	45	69
93% equivalent of $[Fe^{2+}]_o$	$[KMnO_4]$	4.37	21.88
	$[NaHCO_3]$	42	68
95% equivalent of $[Fe^{2+}]_o$	$[KMnO_4]$	4.43	22.16
	$[NaHCO_3]$	40	67
(b) with percentage of $KMnO_4$ as response			
Independent factors		Coded levels in mg/L	
		−1	+1
$[NaHCO_3]$		40	72
$[Fe^{2+}]_o$		5	25
(c) with $[NaHCO_3]$ as response			
Independent factors		Coded levels	
		−1	+1
$[Fe^{2+}]_o$ mg/L		5	25
$[KMnO_4]$ % eqvt of $[Fe^{2+}]_o$		80	95

Table 3.2: Experimental data points used for [KMnO$_4$] as 80% equivalent of [Fe^{2+}] and remaining arsenic as response. All concentrations are in mg/L.

Run	Plot (a)		Plot (b)		Plot (c)	
	Factor A [Fe^{2+}]	Factor B [KMnO$_4$]	Factor A [Fe^{2+}]	Factor B [NaHCO$_3$]	Factor A [KMnO$_4$]	Factor B [NaHCO$_3$]
1	5	3.77	15	59	11.31	77.38
2	15	0.64	29.14	59	3.77	46
3	29.14	11.31	15	77.38	0.64	59
4	15	11.31	0.85	59	18.85	46
5	15	11.31	5	46	21.97	59
6	0.85	11.31	15	40.61	11.31	59
7	25	3.77	5	72	11.31	59
8	15	11.31	15	59	11.31	59
9	5	18.85	25	72	3.77	72
10	15	11.31	15	59	11.31	59
11	15	11.31	25	46	11.31	40.61
12	25	18.85	15	59	18.85	72
13	15	21.97	15	59	11.31	59

Table 3.3: Experimental data points used for [KMnO$_4$] as 85% equivalent of [Fe^{2+}] and remaining arsenic as response. All concentrations are in mg/L.

Run	Plot (d)		Plot (e)		Plot (f)	
	Factor A [Fe^{2+}]	Factor B [KMnO$_4$]	Factor A [Fe^{2+}]	Factor B [NaHCO$_3$]	Factor A [KMnO$_4$]	Factor B [NaHCO$_3$]
1	15	12	5	45	23.31	57.5
2	5	20	0.85	57.5	12	57.5
3	25	20	15	57.5	12	75.17
4	0.85	12	15	57.5	4	70
5	5	4	15	57.5	0.686	57.5
6	15	23.31	5	70	4	45
7	15	12	15	39.82	12	57.5
8	25	4	15	57.5	12	39.82
9	15	12	25	70	12	57.5
10	15	12	25	45	20	70
11	29.14	12	15	57.5	12	57.5
12	15	12	15	75.17	20	45
13	15	0.68	29.14	57.5	12	57.5

Table 3.4: Experimental data points used for [KMnO$_4$] as 90% equivalent of [Fe^{2+}] and remaining arsenic as response. All concentrations are in mg/L.

Run	Plot (g)		Plot (h)		Plot (i)	
	Factor A [Fe^{2+}]	Factor B [KMnO$_4$]	Factor A [Fe^{2+}]	Factor B [NaHCO$_3$]	Factor A [KMnO$_4$]	Factor B [NaHCO$_3$]
1	15	12.6	5	45	12.6	57
2	15	12.6	0.857	57	12.6	57
3	15	12.6	15	57	12.6	57
4	5	21.0	15	40.02	4.2	45
5	15	12.6	29.14	57	12.6	40.02
6	15	24.47	25	45	24.47	57
7	0.857	12.6	15	57	0.72	57
8	15	12.6	5	69	12.6	57
9	29.14	12.6	25	69	21	45
10	25	4.2	15	57	12.6	57
11	15	0.72	15	57	4.2	69
12	25	21	15	57	21	69
13	5	4.2	15	73.97	12.6	73.97

Table 3.5: Experimental data points used for [KMnO$_4$] as 93% equivalent of [Fe^{2+}] and remaining arsenic as response. All concentrations are in mg/L.

Run	Plot (j)		Plot (k)		Plot (l)	
	Factor A [Fe^{2+}]	Factor B [KMnO$_4$]	Factor A [Fe^{2+}]	Factor B [NaHCO$_3$]	Factor A [KMnO$_4$]	Factor B [NaHCO$_3$]
1	15	13.12	5	68	21.88	42
2	15	13.12	15	55	4.37	42
3	25	21.88	15	55	25.50	55
4	29.14	13.12	0.85	55	13.12	55
5	15	25.50	25	42	13.12	73.38
6	0.85	13.12	15	55	13.12	55
7	15	13.12	25	68	13.12	55
8	5	4.37	15	36.61	4.37	68
9	15	13.12	15	55	13.125	36.61
10	15	13.12	29.14	55	13.125	55
11	5	21.88	15	73.38	13.125	55
12	15	0.74	15	55	0.74	55
13	25	4.37	5	42	21.88	68

Table 3.6: Coefficients for the final polynomial equation (**Equation 2.3**) in terms of actual factors:

| Plot (Fig: 3.3)	a_0	a_1	a_2	a_3	a_4	a_5
Plot(a)	3.93048	6.99747×10^{-3}	-0.32851	1.22540×10^{-17}	-2.33249×10^{-4}	6.50773×10^{-3}
Plot(b)	14.87226	6.99747×10^{-3}	-0.36348	-1.86396×10^{-17}	-2.33249×10^{-4}	2.18920×10^{-3}
Plot(c)	14.87226	9.28047×10^{-3}	-0.36348	-2.83114×10^{-17}	-4.10277×10^{-4}	2.18920×10^{-3}
Plot(d)	3.07933	2.12311×10^{-3}	-0.26921	1.06329×10^{-17}	-7.07702×10^{-5}	5.80049×10^{-3}
Plot(e)	13.32329	2.12311×10^{-3}	-0.35643	2.01671×10^{-17}	-7.07702×10^{-5}	2.37588×10^{-3}
Plot(f)	13.32329	2.65388×10^{-3}	-0.35643	3.29912×10^{-17}	-1.10578×10^{-4}	2.37588×10^{-3}
Plot(g)	3.13666	-6.41243×10^{-3}	-0.32594	1.22011×10^{-17}	2.13748×10^{-4}	8.30323×10^{-3}
Plot(h)	18.22300	-6.41243×10^{-3}	-0.54550	5.64051×10^{-18}	2.13748×10^{-4}	4.06858×10^{-3}
Plot(i)	18.22300	-7.63384×10^{-3}	-0.54550	5.75815×10^{-18}	3.02930×10^{-4}	4.06858×10^{-3}
Plot(j)	2.07349	-6.28680×10^{-3}	-0.22162	6.50910×10^{-18}	2.09560×10^{-4}	5.70296×10^{-3}
Plot(k)	10.63540	-6.28680×10^{-3}	-0.33296	3.66400×10^{-17}	2.09560×10^{-4}	2.58658×10^{-3}
Plot(l)	10.63535	-7.17671×10^{-3}	-0.33296	2.06892×10^{-17}	2.73398×10^{-4}	2.58658×10^{-3}
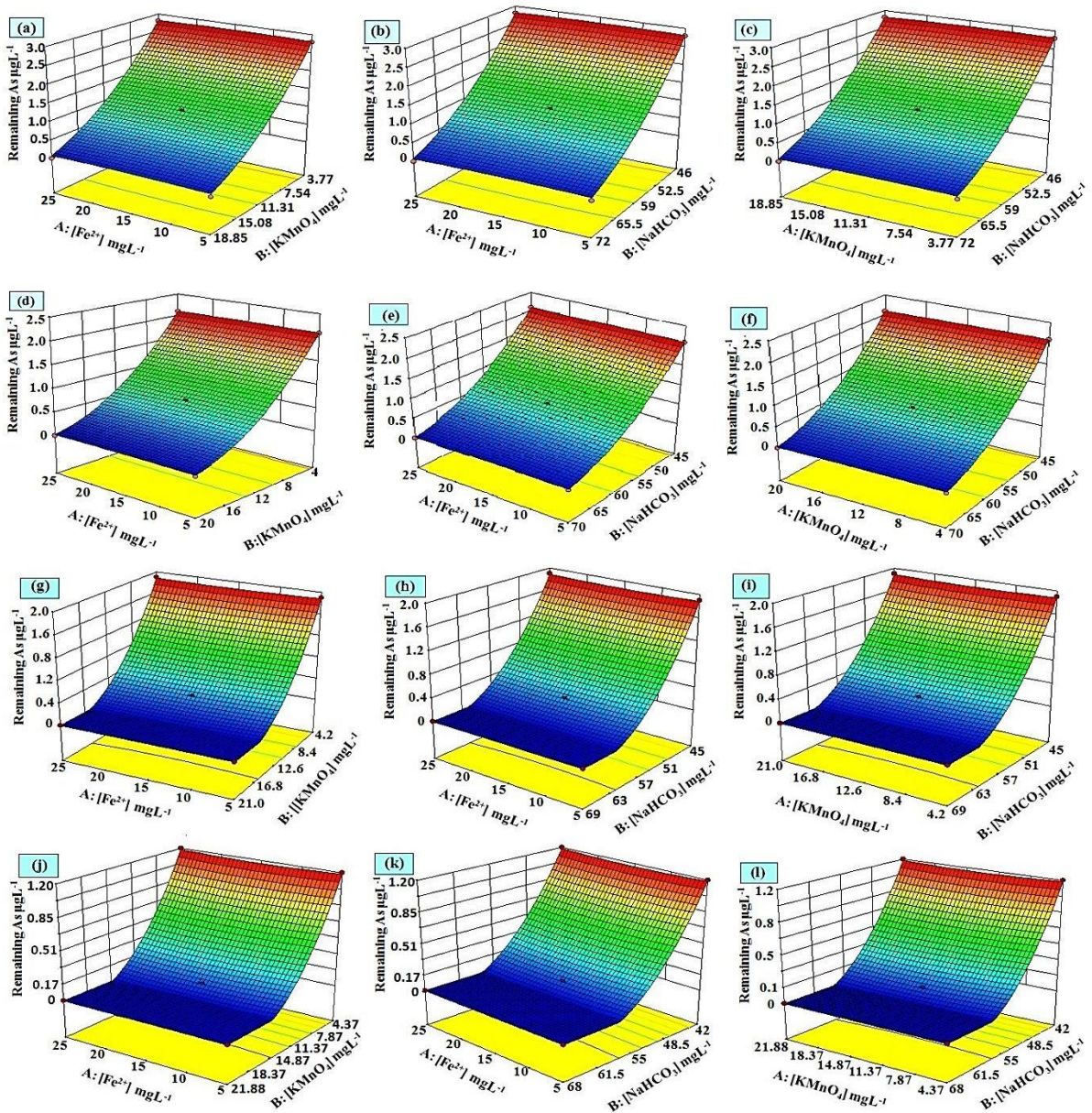
Figure 3.3: 3D plots (plots (a) to (l)) prepared by selecting two independent variables among the three operating variables $[Fe^{2+}]_o$, $[KMnO_4]$, and $[NaHCO_3]$, with remaining arsenic as response in each case.

Table 3.7: The design for CCD for the dose of $KMnO_4$ in percentage equivalent of $[Fe^{2+}]_o$ and the dose of $NaHCO_3$ were taken as response, separately. All concentrations are in mg/L except for $KMnO_4$, which is in percentage equivalent of $[Fe^{2+}]_o$.

Run	[KMnO₄] as response		[NaHCO₃] as response	
	Factor A [NaHCO₃]	Factor B [Fe²⁺]ₒ	Factor A [Fe²⁺]ₒ	Factor B [KMnO₄]
1	40	25	15	87.5
2	56	15	15	87.5
3	56	15	29.141	87.5
4	33.37	15	15	87.5
5	56	15	15	76.893
6	40	5	5	95
7	56	15	15	98.106
8	72	25	0.857	87.5
9	56	15	5	80
10	56	0.857	25	95
11	72	5	15	87.5
12	56	29.14	15	87.5
13	78.62	15	25	80

Plots (a) and (b) of **Figure 3.4** were prepared using **Equation 3.3** and **Equation 3.4** respectively:

$$Y = 90.00 - 8.797 \times 10^{-15} A - 7.43 \times B + 1.905 \times 10^{-14}(A \times B) - 0.051 \times A^2 - 2.35 \times B^2 \qquad (3.3)$$

$$Y = -29.876 + 0.391 \times A + 1.948 \times B + 6.667 \times 10^{-3}(A \times B) + 0.0125 \times A^2 - 0.0133 \times B^2 \qquad (3.4)$$

where, the factors A and B represent the $[NaHCO_3]$ and $[Fe^{2+}]_o$ in **Equation 3.3** and $[Fe^{2+}]_o$ and $[KMnO_4]$ in **Equation 3.4**, respectively.

3.1.3.2. Fit test of CCD model:

Fisher's F-test (Sequential Model Sum of Squares [Type I]) of the 3D plots prepared by CCD of RSM gave the confirmation of the fitting of the quadratic model. From this test we knew the significant terms of each plot. A p-value or prob > F of less than 0.0500 is the indication of significant terms. For quadratic model of all the 3D plots the p-value was found as <0.0500. So, this model has been recommended by the Fit test for analysis of variance (ANOVA).

ANOVA analysis of response surface quadratic model for all the 3D plots shown in **Figure 3.3** and in **Figure 3.4** are given in **Table 3.8**. The model F-values obtained from ANOVA analysis for plots of the doses of $KMnO_4$ as 80%, 85%, 90%, 93% equivalent of $[Fe^{2+}]_o$ indicating the model to be significant. A model F-value of 4136.41 and 719.78 for the plots of optimized doses of $KMnO_4$ and for optimized dose of $NaHCO_3$ respectively also suggests that model is significant. The values of "Prob> F", i.e., p-value less than 0.0500 indicate the models to be significant. ANOVA of the plots of **Figure 3.3** and **3.4** gives a highly reliable value of R^2, adjusted-R^2 and predicted-R^2 for quadratic model of the plots presented in **Table 3.9**. Adequate Precision measures the signal to noise ratio. A ratio greater than 4 is desirable. All the Adequate Precision of our models is greater than 4 and therefore these models can be used to navigate the present design space. The quadratic model has been validated by diagnostics case studies.

The residuals in the normal plots fall on a straight line (shown in **Figure 3.5**) indicating that the errors are distributed normally.
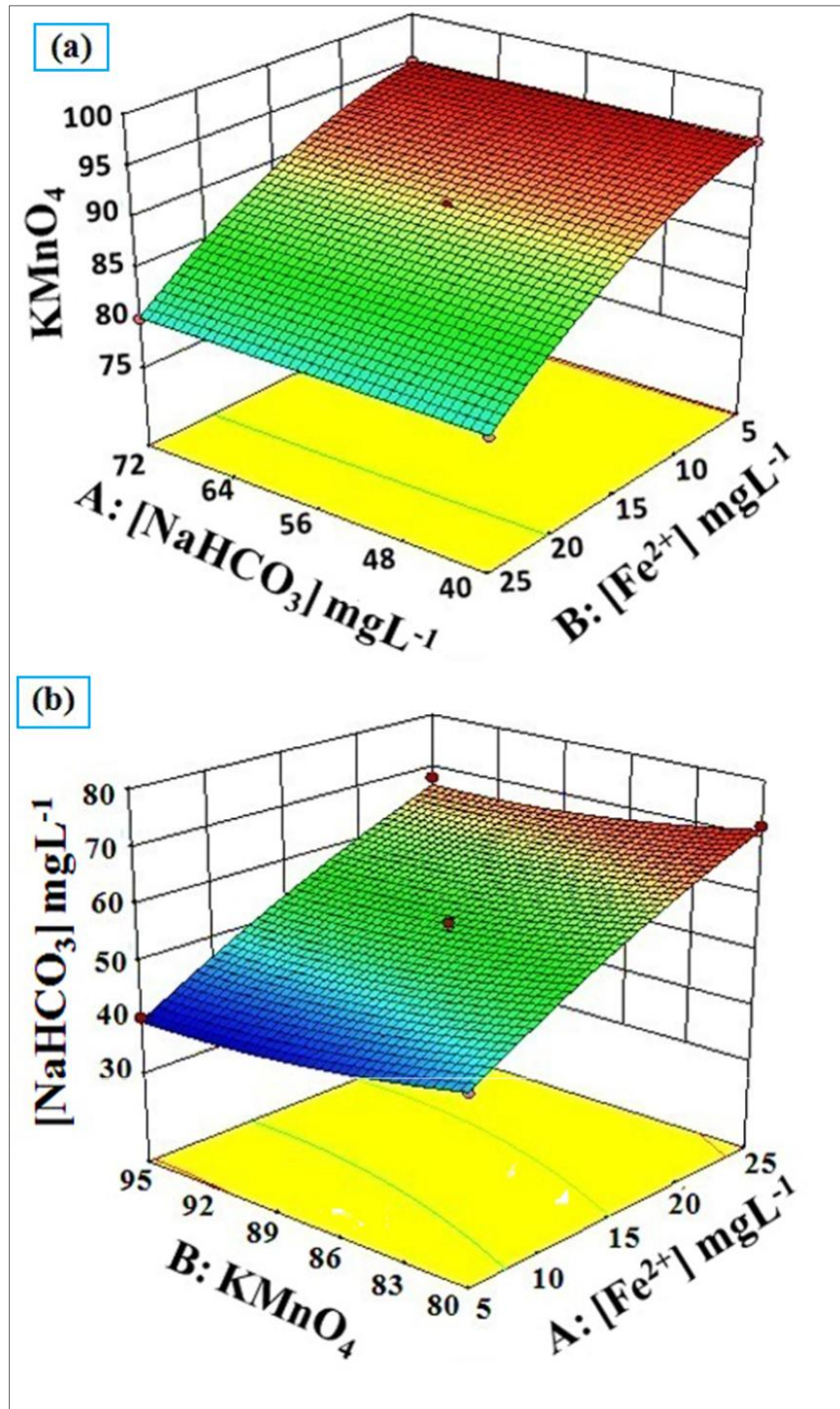
Figure 3.4: Plot of (a) required doses of KMnO$_4$ in percentage equivalent of [Fe^{2+}]$_o$ with variation of [Fe^{2+}]$_o$ and [NaHCO$_3$] and (b) required doses of NaHCO$_3$ with variation of [Fe^{2+}]$_o$ and KMnO$_4$ in percentage equivalent of [Fe^{2+}]$_o$ for removal of arsenic from 100 μg/L to less than 1 μg/L.

Table 3.8: Sum of squares with F-value and P-value of the models of 3D plots obtained from ANOVA.

3D plots for experimental results with different operating variables:						
Response	$[KMnO_4]^*$	Operating varibles	Sum of square	F-value	P-value	Significance
Remaining [As]	80%	$[Fe^{2+}]_o$ & $[KMnO_4]^*$ $[Fe^{2+}]_o$ & $[NaHCO_3]$ $[KMnO_4]^*$ & $[NaHCO_3]$	9.38	431.17	< .0001	√
Remaining [As]	90%	$[Fe^{2+}]_o$ & $[KMnO_4]^*$ $[Fe^{2+}]_o$ & $[NaHCO_3]$ $[KMnO_4]^*$ & $[NaHCO_3]$	5.35	2668.89	< .0001	√
Remaining [As]	93%	$[Fe^{2+}]_o$ & $[KMnO_4]^*$ $[Fe^{2+}]_o$ & $[NaHCO_3]$ $[KMnO_4]^*$ & $[NaHCO_3]$	4.93	269.61	< .0001	√
Remaining [As]	95%	$[Fe^{2+}]_o$ & $[KMnO_4]^*$ $[Fe^{2+}]_o$ & $[NaHCO_3]$ $[KMnO_4]^*$ & $[NaHCO_3]$	2.13	121.15	< .0001	√
3D plots for the required doses of $KMnO_4^*$ and $NaHCO_3$ with different operating variables:						
Response		Operating variables	Sum of square	F-value	P-value	Significance
Required dose of $KMnO_4^*$		$[Fe^{2+}]_o$ and $[NaHCO_3]$	422.79	4136.41	< .0001	√
Required dose of $NaHCO_3$		$[Fe^{2+}]_o$ and $[KMnO_4]^*$	771.84	719.78	<0.0001	√

*In percentage equivalent of $[Fe^{2+}]_o$.

Table 3.9: The R^2, adjusted R^2 and predicted R^2 values of the 3D plots obtained by analysis of variance (ANOVA) along with standard deviation (SD), mean, C.V.%, precision and adequate precision (AP).

		SD	0.17	R^2	0.9850
Figure 3.3	Mean	1.26	Adjusted R^2	0.9743
Plots (a), (b) and (c)	C.V.%	13.27	Predicted R^2	0.8933
	Precision	1.39	AP	31.046
	SD	0.020	R^2	0.9996
Figure 3.3	Mean	0.76	Adjusted R^2	0.9992
Plots (d), (e) and (f)	C.V.%	2.64	Predicted R^2	0.9960
	Precision	0.021	AP	150.660
	SD	0.060	R^2	0.9956
Figure 3.3	Mean	0.49	Adjusted R^2	0.9919
Plots (g), (h), (i)	C.V.%	12.30	Predicted R^2	0.9605
	Precision	0.20	AP	45.859
	SD	0.059	R^2	0.9902
Figure 3.3	Mean	0.26	Adjusted R^2	0.9820
Plot (j), (k) and (l)	C.V.%	22.94	Predicted R^2	0.9126
	Precision	0.19	AP	30.046
	SD	0.14	R^2	0.9997
Figure 3.4	Mean	87.92	Adjusted R^2	0.9995
Plot (a)	C.V.%	0.16	Predicted R^2	0.9974
	Precision	1.09	AP	200.116
Figure 3.4	SD	0.46	R^2	0.9986
Plot (b)	Mean	55.91	Adjusted R^2	0.9972
	C.V.%	0.83	Predicted R^2	0.9445
	Precision	42.89	AP	91.419
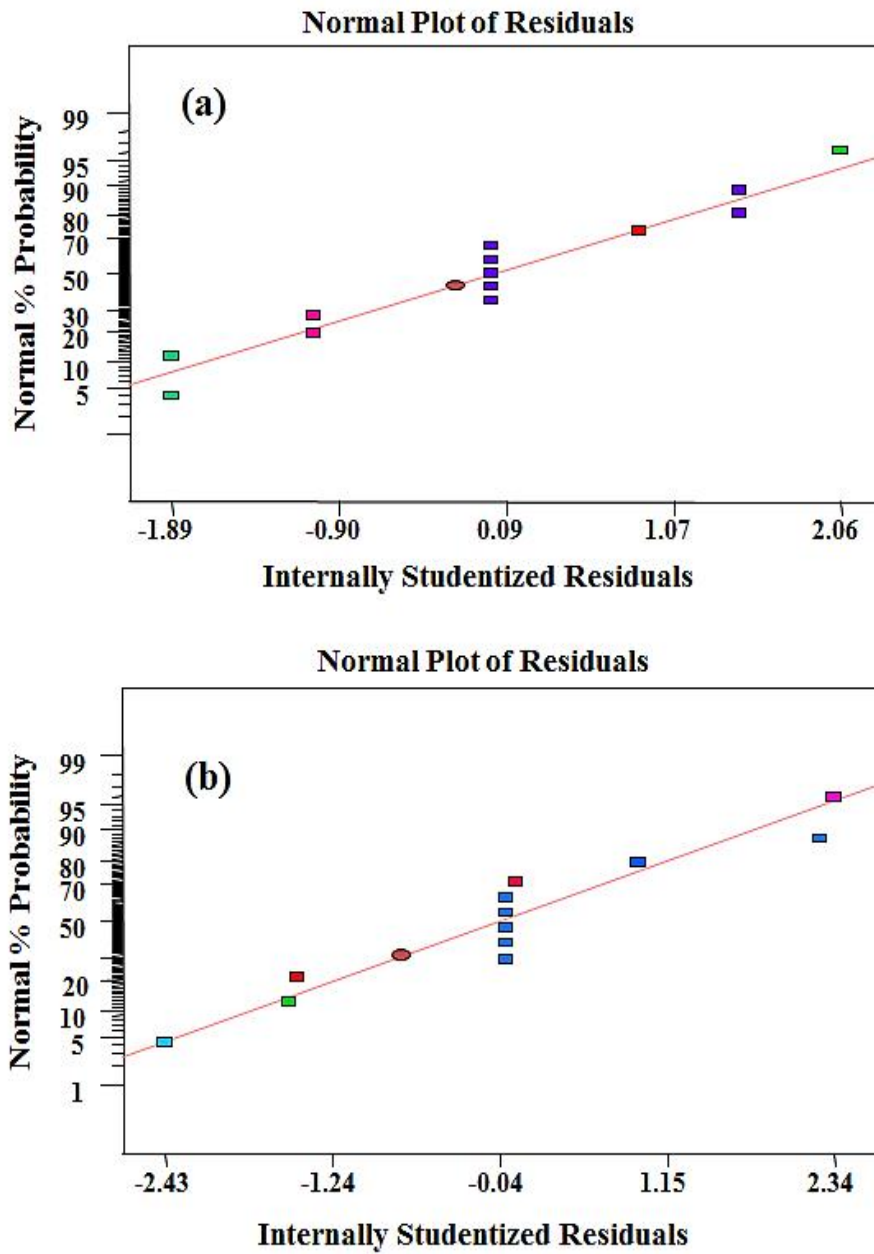
Figure 3.5: Studentized plots showing normal% probability versus internally studentized residuals for models with (a) $KMnO_4$ and (b) $NaHCO_3$ as response

Table 3.10: The predicted and observed values of the response for [KMnO$_4$] as 80% equivalent of [Fe^{2+}]

	Remaining As concentration µg/L					
	From plot (a)		From plot (b)		From plot (c)	
Run	Predicted	Observed	Predicted	Observed	Predicted	Observed
1	2.8136	2.8	1.10	1.1	0.0796	0
2	2.9870	3.7	1.10	1.1	2.8136	2.8
3	1.10	1.1	0.079	0	1.10	1.1
4	1.10	1.1	1.10	1.1	2.8136	2.8
5	1.10	1.1	2.8136	2.8	1.10	1.1
6	1.10	1.1	2.89	3.3	1.10	1.1
7	2.8136	2.8	0.0796	0	1.10	1.1
8	1.10	1.1	1.1	1.1	1.10	1.1
9	0.0796	0	0.0796	0	0.0796	0
10	1.10	1.1	1.10	1.1	1.10	1.1
11	1.10	1.1	2.8136	2.8	2.976	3.2
12	0.079	0	1.10	1.1	0.0796	0
13	0.079	0	1.10	1.1	1.10	1.1

Table 3.11: The predicted and observed values of the response for [KMnO$_4$] as 85% equivalent of [Fe^{2+}]:

	Remaining As concentration µg/L					
	From plot (d)		From plot (e)		From plot (f)	
Run	**Predicted**	**Observed**	**Predicted**	**Observed**	**Predicted**	**Observed**
1	0.70	0.7	2.104	2.1	0.70	0.7
2	0.024	0	0.70	0.7	0.70	0.7
3	0.024	0	0.70	0.7	0.024	0
4	0.70	0.7	0.70	0.7	0.024	0
5	2.104	2.1	0.70	0.7	0.024	0.7
6	0.024	0	0.024	0	2.104	2.1
7	0.70	0.7	3.134	3.7	0.70	0.7
8	2.104	2.1	0.70	0.7	2.786	2.99
9	0.70	0.7	0.024	0	0.70	0.7
10	0.70	0.7	2.104	2.1	0.024	0
11	0.70	0.7	0.70	0.7	0.70	0.7
12	0.70	0.7	0.024	0	2.104	2.1
13	2.978	3.4	0.70	0.7	0.70	0.7

Table 3.12: The predicted and observed values of the response for [KMnO$_4$] as 90% equivalent of [Fe^{2+}]:

	Remaining As concentration µg/L					
	From plot (g)		From plot (h)		From plot (i)	
Run	predicted	Observed	predicted	Observed	Predicted	Observed
1	0.3	0.3	1.719	1.9	0.3	0.3
2	0.3	0.3	0.3	0.3	0.3	0.3
3	0.3	0.3	0.3	0.3	0.3	0.3
4	0.033	0	1.976	2.3	1.86	1.9
5	0.3	0.3	0.3	0.3	1.95	2.2
6	0.033	0	1.719	1.9	0.3	0.3
7	0.3	0.3	0.3	0.3	0.3	0.3
8	0.3	0.3	0.044	0	0.3	0.3
9	0.3	0.3	0.044	0	1.86	1.9
10	1.658	1.9	0.3	0.3	0.3	0.3
11	1.98	2.1	0.3	0.3	0.038	0
12	0.033	0	0.3	0.3	0.038	0
13	1.658	1.9	0.044	0	0.038	0

Table 3.13: The predicted and observed values of the response for [KMnO₄] as 93% equivalent of [Fe^{2+}]:

	Remaining As concentration µg/L					
	From plot (j)		**From plot (k)**		**From plot (l)**	
Run	**predicted**	**Observed**	**Predicted**	**Observed**	**Predicted**	**Observed**
1	0.10	0.1	0.0715	0	1.187	1.2
2	0.10	0.1	0.10	0.1	1.187	1.2
3	0.0715	0	0.10	0.1	0.10	0.1
4	0.134	0.1	0.135	0.1	0.10	0.1
5	0.0715	0	1.187	1.2	0.0715	0
6	0.10	0.1	0.10	0.1	0.10	0.1
7	0.10	0.1	0.0715	0	0.10	0.1
8	1.187	1.2	1.78	1.67	0.0715	0
9	0.10	0.1	0.10	0.1	1.68	1.73
10	0.10	0.1	0.10	0.1	0.10	0.1
11	0.0715	0	0.002	0	0.10	0.1
12	3.124	3.2	0.10	0.1	0.124	0.1
13	1.187	1.2	1.187	1.2	0.0715	0

Table 3.14: The predicted and experimental doses of KMnO$_4$ (in percentage equivalent of [Fe^{2+}]) and NaHCO$_3$ (in mg/L) as responses respectively with remaining arsenic less than 1 µg/L

	For KMnO$_4$ (%)		For NaHCO$_3$ (mg/L)	
Run	**Predicted**	**Experimental**	**Predicted**	**Experimental**
1	80.21	80	56	56
2	90	90	56	56
3	90	90	67.51	70
4	90	90	56	56
5	90	90	58.53	57
6	94.78	95	39.43	40
7	90	90	56.01	54
8	80.21	80	58.78	58
9	90	90	46.23	46
10	95.34	95	66.62	68
11	94.78	95	56	56
12	78.73	75	56	56
13	90	90	71.43	72

3.1.3.2. Findings:

The predicted and experimentally observed values of remaining arsenic concentration when [KMnO$_4$] was 80%, 85%, 90% and 93% equivalent of [Fe^{2+}]$_o$ were determined and presented in **Table 3.10-3.13**, sequentially. The experimental values for the response were all zero, without any high or low level, when [KMnO$_4$] was 95% equivalent of [Fe^{2+}]$_o$. From **Table 3.10-3.13** we can determine the arsenic removal efficiency i.e. remaining arsenic for 13 experimental run. Each experimental run has two variables among three major operating variables namely coexisting iron concentration, [Fe^{2+}]$_o$, [KMnO$_4$], and [NaHCO$_3$]. Values of

concentrations of the selected variables in CCD of RSM for each experimental run are given in the **Table 3.2-3.5**. Accordingly by studying the **Table 3.2-3.5** and **Table 3.10-3.13** we can determined the remaining arsenic concentration with respect to the two major operating variables among $[Fe^{2+}]$ (mg/L), $KMnO_4$ (in % eqvt of $[Fe^{2+}]_o$) and $NaHCO_3$ [mg/L] presented in **Figure 3.3**.

After knowing the remaining arsenic concentration with respect to two of three variables, namely, the coexisting iron, $KMnO_4$, and $NaHCO_3$ we can evaluate the optimized dose of $KMnO_4$ in % equivalent of $[Fe^{2+}]_o$ and $NaHCO_3$ in mg/L when removal is found to less than 1 µg/L from 100 µg/L by further RSM analysis, taking:

(a) dose of $KMnO_4$ in % equivalent of $[Fe^{2+}]_o$ as response when independent variables are $[Fe^{2+}]_o$ and $[NaHCO_3]$ in mg/L and,

(b) $[NaHCO_3]$ in mg/L as response when independent variables are the dose of $KMnO_4$ in % equivalent of $[Fe^{2+}]_o$ and $[Fe^{2+}]_o$ in mg/L, respectively.

Accordingly the RSM analysis (**Table 3.7** and **Figure 3.4**) shows that if $[Fe^{2+}]_o$ present in water are 0.857, 5, 10, 15, 20, 25, and 29.14 mg/L then the required doses of $KMnO_4$ as percentage of equivalent of $[Fe^{2+}]_o$ will be 95.34%, 95%, 92.84%, 90%, 85%, 80.21%, and 78.73% respectively. **Table 3.14** shows a close correlation between the predicted and the experimental doses of $KMnO_4$ and $NaHCO_3$ with respect to coexisting iron, Fe^{2+} concentration. In laboratory experiment added dose of $KMnO_4$ was 95%, 93%, 90%, 85%, 80% for $[Fe^{2+}]_o$ as 0–5, 5–10, 10–15, 15–20, and 20–25 mg/L, respectively, to remove arsenic from initial 100 µg/L to less than 1 µg/L.

The RSM analysis (**Table 3.7** and **Figure 3.4**) also shows that if $[Fe^{2+}]_o$ present in water are 5, 10.27, 15, 20.09, 25 mg/L then the required doses of $NaHCO_3$ are 39.43, 48.03, 56, 62.20, 71.43, respectively. For practical purpose we rounded off the dose of $NaHCO_3$ to 40, 48, 56, 61, and 72 mg/L for initial iron concentrations of 5, 10, 15, 20, and 25 mg/L, respectively. Thus, the predicted values of remaining arsenic concentration along with doses of $KMnO_4$ in percentage equivalent of $[Fe^{2+}]_o$ and doses of $NaHCO_3$ obtained from the CCD design of RSM fairly correlate with the experimental results as shown in **Table 3.14**. Therefore, our optimization of the required doses of $KMnO_4$ and $NaHCO_3$ with respect $[Fe^{2+}]_o$ is good and is also capable of predicting the doses outside the experimental range of 5 mg/L to 25 mg/L of $[Fe^{2+}]_o$. Accordingly we can use the RSM optimized doses of $KMnO_4$ and $NaHCO_3$ in field application to remove arsenic below 1 µg/L on the basis of coexisting

iron concentration and thereby lowering the cost of the OCOP method utilizing coexisting iron.

3.1.3. Field study:

The field trial experiments were conducted with 32 households and 8 schools of some As-contaminated areas of Nagaon, Mangaldoi, Lakhimpur and Jorhat in Assam, India. The doses of $KMnO_4$ in percentage equivalent of coexisting (or initial iron) concentration, and $NaHCO_3$ were added which were obtained from the optimization by RSM as shown in **Figure 3.6**. The field trial was carried out with both 20 L households and 200 L for small community filters with groundwater from tube well sources contaminated with both arsenic and iron in the selected areas. The initial concentrations of arsenic and iron in the groundwater from tube well sources were in the ranges of 284–25 mg/L and 2.9–23.0 mg/L, respectively presented in **Table 2.2** of **Section 2.2.1.3**. Arsenic and iron removal efficiencies were examined by AAS in these installed units time to time. Results of remaining arsenic, remaining iron, remaining manganese concentration, along with final pH of the treated water after the field experiment by the present modified OCOP method to remove arsenic and iron from tube well water of the selected areas is presented in **Figure 3.7, 3.7, 3.9, and 3.10**, respectively.
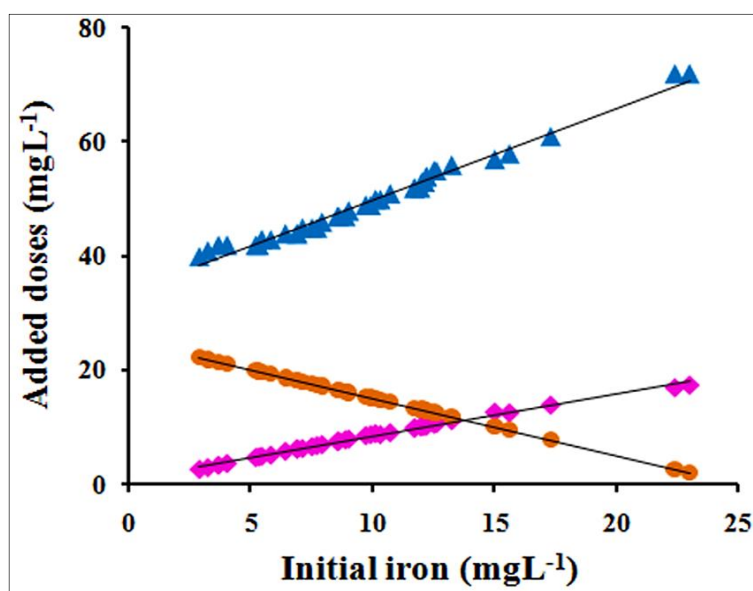
Figure 3.6: The doses of $KMnO_4$ and $FeCl_3$ used in field trial at 32 households and 8 schools at different districts of Assam to remove arsenic below 1 μ/L. Symbols: ▲ - $NaHCO_3$, ● - $FeCl_3$ and ♦ - $KMnO_4$.
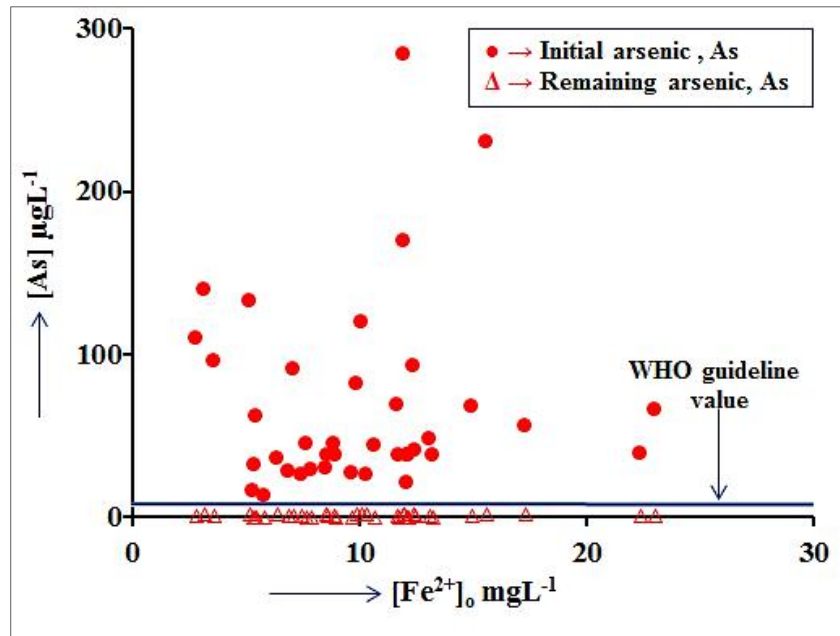
Figure 3.7: Plot of initial arsenic and remaining arsenic with respect to initial iron concentration. (Average % of error for triplicate experiment = 0.58%).
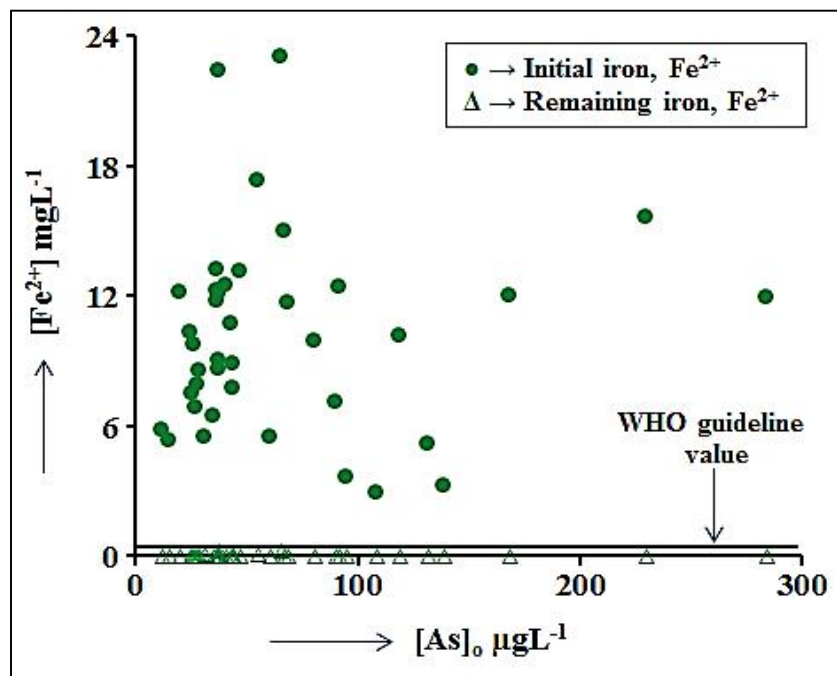
Figure 3.8: Plot of initial and remaining iron with respect to initial arsenic concentration.
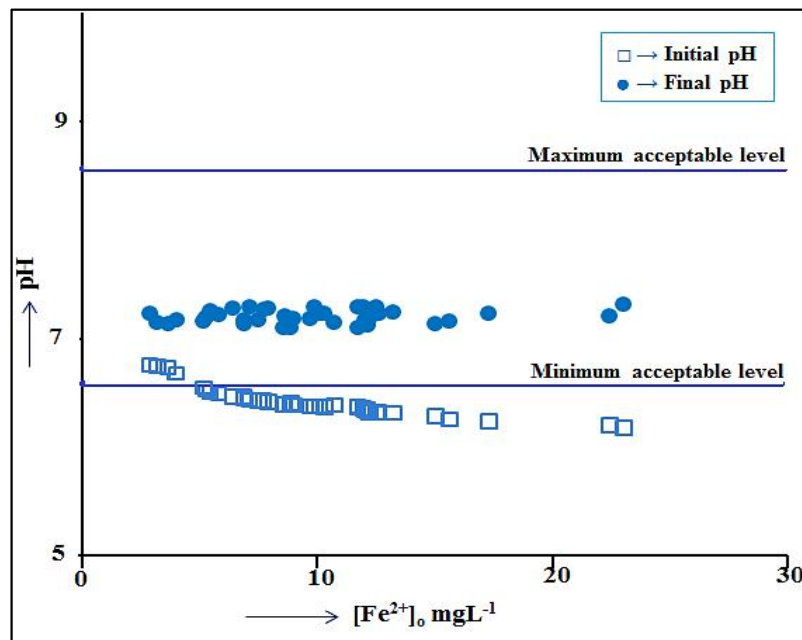
(Average % of error for triplicate experiment = 1.12%).
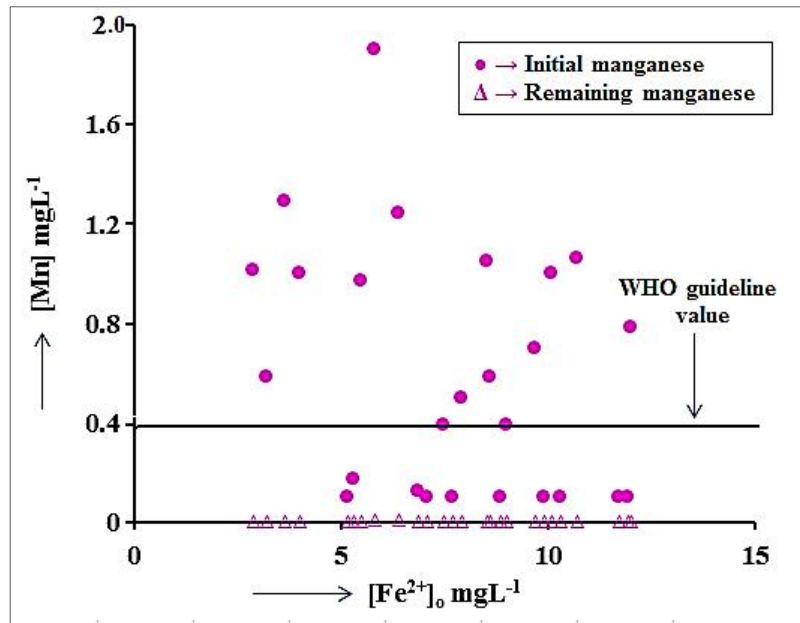
Figure 3.9: plot of initial and remaining manganese with respect to initial iron concentration. (Average % of error for triplicate experiment = 1.03%)

Figure 3.10: plot of initial and final pH with respect to initial iron concentration.

(Average % of error for triplicate experiment = 0.05%)

Figure 3.7 presents the removal of arsenic from various initial arsenic concentrations with respect to coexisting iron concentration of field trial experiments done in some arsenic effected areas of Assam. From **Figure 3.7** it is seen that arsenic was satisfactorily removed from initial concentration of about 284-25 µg/L to less than 2 µg/L. Along with arsenic, iron was also removed from initial concentrations in the range of 23.0–2.9 mg/L to less than 0.01 mg/L by the present method which is presented in **Figure 3.8**. Thus, the present modified OCOP method can simultaneously lower the concentrations of arsenic and iron from contaminated groundwater to levels about ten times lower than the respective guideline values of 10 µg/L and 0.3 mg/L prescribed by the WHO [55]. It can be mentioned here that Mn concentrations also was also lowered to <0.02 mg/L which is much below WHO guideline value of 0.1 mg/L as can be seen from **Figure 3.9** [55]. The Mn concentration did not increase after the treatment despite the use of $KMnO_4$ since Mn was precipitated as MnO_2 in the near neutral alkaline condition provided by the added $NaHCO_3$. **Figure 3.10** shows that the measured pH values of the treated water were in the range of 7.00– 7.30, which is suitable for drinking purposes. The mechanism of arsenic removal and the nature of the solid sludge of the present modified method are expected to be same as that of the OCOP method [218].

Some more water quality parameters of the water were measured before and after the treatment and were found to be within the permissible limits presented in **Table 3.15**. From **Table 3.15** it is observed that water quality parameters are well controlled by our modified OCOP method below the maximum acceptable limits recommended by WHO. Accordingly we will get suitable drinking water by treatment of groundwater sources by our present modified OCOP method. So we conclude that our modified OCOP method with optimized doses of $KMnO_4$ and $NaHCO_3$ and $FeCl_3$ dose as (= 25 mg/L - $[Fe^{2+}]_o$) is far better process which can remove arsenic and iron below 1µg/L and 0.01mg/L respectively with lowering the cost by utilizing coexisting iron, Fe^{2+}.

Table 3.15: Some average relevant water quality parameters of the water measured before and after the treatment of synthetic water in laboratory experiment and groundwater in field application.

Water quality parameters	WHO guideline value	Groundwater		Synthetic water		Units
		Before treatment	After treatment	Before treatment	After treatment	
Chloride (Cl⁻)	250	5.6	11.9	2.3	4.6	mg/L
Nitrate (NO₃⁻)	50	<1.0	<1.0	nd*	Nd	mg/L
Fluoride (F⁻)	1.5	0.34	0.31	0.2	0.2	mg/L
Sulphate (SO_4^{2-})	500	7.8	7.5	6.4	6.2	mg/L
Phosphate as P (PO_4^{2-})	ns**	<0.003	<0.003	Nd	Nd	mg/L
Sodium (Na⁺)	Ns	5.73	16.4	4.71	13.34	mg/L
Potassium (K⁺)	Ns	10.9	8.7	7.7	6.7	mg/L
Manganese (Mn^{2+})	0.10	0.095	0.0014	0.002	0.001	mg/L
Calcium (Ca^{2+})	75	0.88	0.80	0.72	0.64	mg/L
Magnesium (Mg^{2+})	Ns	2.11	1.34	0.978	0.078	mg/L
Silica (SiO_2)	Ns	4.37	2.78	Nd	Nd	mg/L
Dissolved oxygen(DO)	Ns	81.4	76.6	83.45	79.23	%
Dissolved solids	600	132	171	96	123	mg/L

*Not done, **Not specified, Average % of error for triplicate experiment = 1.08%.

3.1.4. Feasibility of this modified OCOP method:

One can see from **Figure 3.6** that there is about 5/4 mg/L decrease in the required dose of ferric chloride for each mg/L increase in the dose of potassium permanganate, required to oxidise the existing ferrous iron to utilize of the later for the coagulation purpose. There is a small increase in the required dose of $NaHCO_3$ with increase in the concentration of the co-existing iron. However, as such one has to add higher dose of $NaHCO_3$ to correct the pH to the acceptable range as the initial pH decreases with increase in the $[Fe^{2+}]_0$. Thus, we can ignore the increase in the cost due to increase in the dose of $NaHCO_3$. An estimate considering the current Indian market prices of bulk $NaHCO_3$, $KMnO_4$ and $FeCl_3$ as USD 0.5/kg, 2.5/ kg and 1/kg, and their doses required for 1 m^3 of water as 100 g, 0.5 g and 25 g, respectively, the cost of the OCOP turns out to be $\approx$USD 0.077/m^3 of water with coexisting $[Fe^{2+}]_0$ less than 1 mg/L. For 25 mg/L coexisting $[Fe^{2+}]_0$, the $KMnO_4$ dose has to be increased by 23.5 g/m^{-3} in the OCOP method to oxidise Fe^{2+}. This increases the cost of the OCOP method by $\approx$USD 0.059 per m^3 to $\approx$USD 0.126 per m^3 of treated. In MOCOP, $FeCl_3$ is not required for water with >25 mg/L coexisting $[Fe^{2+}]_0$. The saving for 25 g/m^{-3} $FeCl_3$ is $\approx$USD 0.025 per m^3 giving a total chemical cost of present OCOP as $\approx$USD 0.10 per m^3. Thus, with competing chemical cost with other coagulation methods, the present OCOP removes arsenic more efficiently to <2 µg/L along with coexisting iron. The present OCOP also saves almost 20% of the cost of earlier OCOP for water with 25 mg/L coexisting iron through saving in terms of the $FeCl_3$ dose.

Arsenic removal comparable to the present method has been reported with various methods, including oxidation-coagulation-adsorption, but they vary widely in terms of the targets and conditions under which the removal is done [266]. For example, Guibai et al. reported removal of As^{3+} below 10 µg/L by treatment with $FeCl_3$ and $KMnO_4$ followed by ultrafiltration [267]. Meng and Korfiatis reported requirement of about 20 mg/L of Fe^{3+} to reduce arsenic to less than 50 µg/L from arsenic contaminated ground-water [268]. 100 mg/L of $FeCl_3$ and 1.4 mg/L of $KMnO_4$ is reported to reduce arsenic contents of treated water below 20 µg/L from initial groundwater arsenic of 375–640 µg/L [269]. The removal of arsenic to about ten times lower than the WHO guideline value of 10 µg/L by the present OCOP method is important in view of the WHO advice to remove arsenic to as low as possible given the reported carcinogenic effect of arsenic at concentrations even below the guideline value [55].

3.2. Simultaneous removal of As, Fe and Mn by OCOP*:

In this section we address removal of manganese by the OCOP along with arsenic and iron.

3.2.1. Initial laboratory experiments:

A series of OCOP experiments for RSM optimization of the doses of $NaHCO_3$, $FeCl_3$ and $KMnO_4$ was performed as described in the experimental procedure in section 2.2.2. The experiments were carried out in 1 L mugs containing synthetically prepared contaminated water with a fixed initial arsenite ion concentration ($[As^{3+}]_0$) at 100 μg/L. The initial iron ion concentration ($[Fe^{2+}]_0$) was varied from 1 mg/L to 8 mg/L and the initial manganese ion concentration ($[Mn^{2+}]_0$) was varied from 0.5 mg/L to 5.0 mg/L with an interval concentration of 0.5 mg/L [248].

Here aqueous 9% $NaHCO_3$ solution was added dropwise to each solution to and pH of the water is found to ≈ 8.5. After that aqueous $KMnO_4$ solution was added in percentage equivalent of initial iron concentration, $[Fe^{2+}]_0$ from 30% to 100%. Then dose of $FeCl_3$ as $[Fe^{3+}]$ was taken as equal to (8.6–$[Fe^{2+}]_0$) in mg/L. Then, aqueous $NaHCO_3$ was added again to adjust the final pH at ≈7.3. The water was stirred gently with a glass rod during addition of $NaHCO_3$, $KMnO_4$ and $FeCl_3$. The amount of total added $NaHCO_3$ in mg/L was noted. After the dosing the water was allowed to coagulate and settle down for two hour. The filtered water samples were preserved for analysis by AAS to determine the remaining concentration of Mn, As, Fe and other water quality parameters.

3.2.1.1. Observation:

Figure 3.11 shows the remaining total arsenic concentration as a function of increasing $KMnO_4$ dose in % equivalent of initial or coexisting iron concentration, $[Fe^{2+}]_0$ with varying concentrations of coexisting (initial) ferrous iron ion, $[Fe^{2+}]_0$ and manganous ion, $[Mn^{2+}]_0$ in the range 1 - 8 mg/L and 0.5 – 5.0 mg/L, respectively [248].

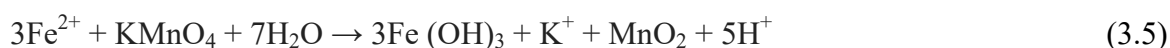We observed an increase in the removal of arsenic with increase in $[Fe^{2+}]_0$ and $[Mn^{2+}]_0$ as well as with increase in the dose of $KMnO_4$ as $FeCl_3$ alone cannot remove As^{3+} efficiently [270]. The observed increase in the removal of arsenic with increasing $[Fe^{2+}]_0$ at fixed $[Mn^{2+}]_0$ indicates increased formation of iron coagulates after conversion of the more and more coexisting Fe^{2+} into Fe^{3+} after addition of $KMnO_4$.

But the removal of arsenic with increasing $[Mn^{2+}]_0$ at fixed $[Fe^{2+}]_0$ may be ascribed to increased adsorption of arsenic on solid MnO_2 precipitates [271, 272] formed due to oxidation of Mn^{2+} ions by $KMnO_4$ and catalysis of the oxidation of As^{3+} to As^{5+} by MnO_2.

It was observed that remaining total [As], $[Mn^{2+}]$ and $[Fe^{2+}]$ after the treatment were below 1 µg/L, 0.009 mg/L and 0.03 mg/L down from their initial concentrations of 100 µg/L, 5 mg/L and 8 mg/L, respectively [248]. In **Tables 3.16** and **3.17** presents the experimentally found minimum doses of $KMnO_4$ in % equivalent of $[Fe^{2+}]_0$ and $NaHCO_3$ in mg/L with which arsenic was removed to below 1 µg/L from initial 100 µg/L by the modified OCOP method in laboratory. These data were used for RSM analysis to optimize the doses of $NaHCO_3$, $KMnO_4$, and $FeCl_3$ for removal of As, Mn and Fe below 1 µg/L, 0.009 mg/L and 0.03 mg/L respectively.

The dose of $FeCl_3$ was taken as equal to $(8.6 – [Fe^{2+}]_0)$ in mg/L [218]. This empirical equation used for deciding the doses of $FeCl_3$ for the design experiment, viz., $[Fe^{3+}] = (8.6 - [Fe^{2+}]_0)$ in mg/L as Fe was obtained experimentally and has been validated by results of arsenic removal by our former research group Bordoloi, et al. [218]. This 8.6 mg/L was the dose of $FeCl_3$ as Fe^{3+} in mg/L in OCOP and there is no need further addition of $FeCl_3$ when coexisting $[Fe^{2+}]_0$ is above 8.6 mg/L because this $[Fe^{2+}]_0$ is expected to provide Fe^{3+} ions equal to the dose of $FeCl_3$ in OCOP. $KMnO_4$ produces water insoluble MnO_2 from its reactions with Fe^{2+}, Mn^{2+} and AsO_3^{3-} in the mild alkaline condition provided by $NaHCO_3$ [267] as follows:
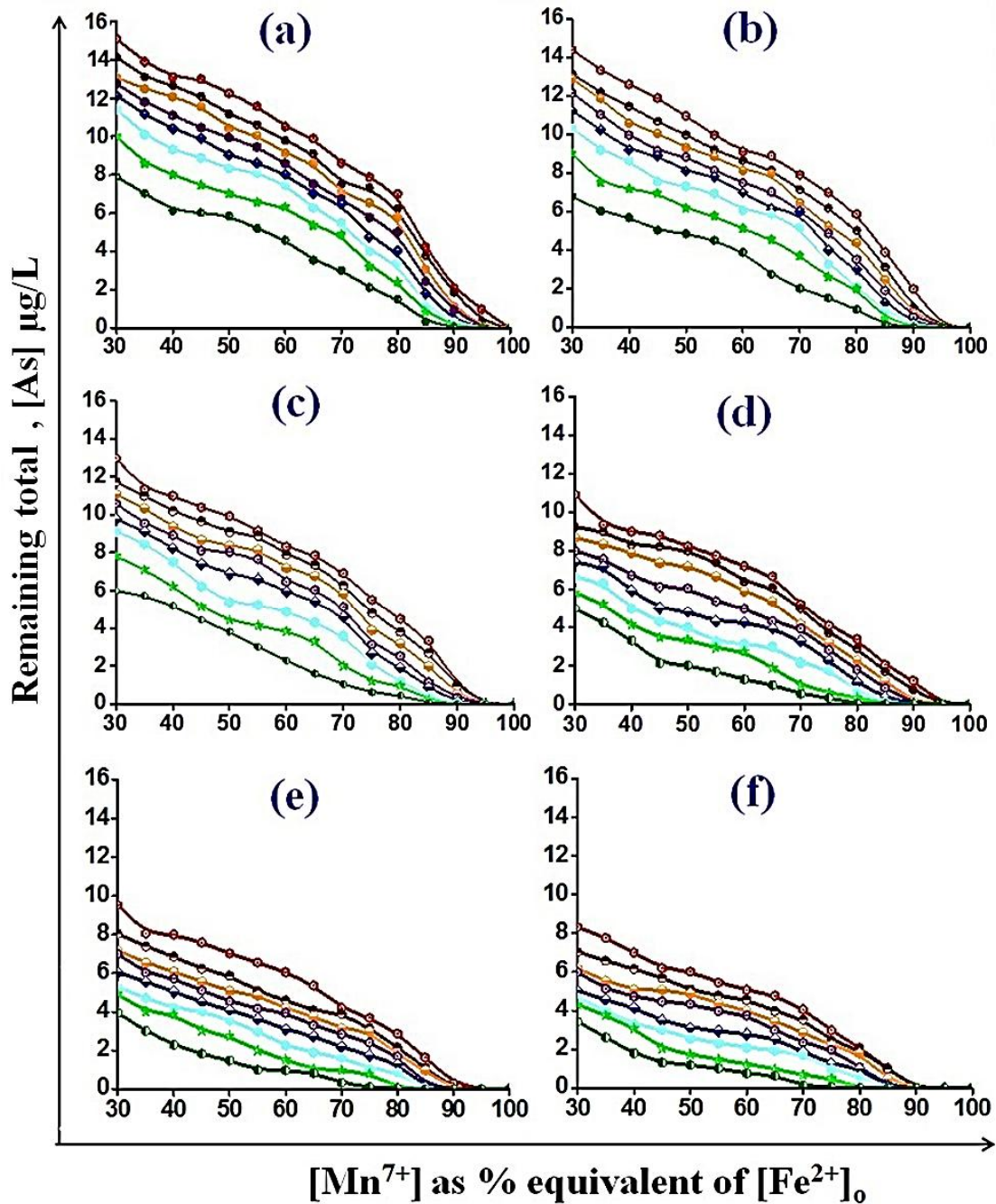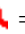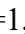
$$3Fe^{2+} + KMnO_4 + 7H_2O \rightarrow 3Fe(OH)_3 + K^+ + MnO_2 + 5H^+ \tag{3.5}$$

$$Mn^{2+} + KMnO_4 \rightarrow 2MnO_2 + K^+ \tag{3.6}$$

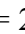$$3H_3AsO_3 + 2KMnO_4 + 4OH^- \rightarrow 3HAsO_4^{2-} + 2MnO_2 + 5H_2O + 2K^+ \tag{3.7}$$
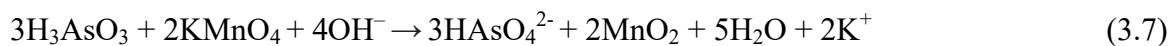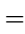
Figure 3.11: Plots of remaining total [As] vs. $[Mn^{7+}]$ in percentage equivalent of $[Fe^{2+}]_0$ for varying $[Mn^{2+}]_0$ and $[Fe^{2+}]_0$. Dose of $NaHCO_3$ was added as per required to adjust the pH of treated water to 7.0–7.3 and dose of $FeCl_3 = (8.607–[Fe^{2+}]_0)$ in mg/L. $[Mn^{2+}]_0/(mg/L)$: (a) = 0.5, (b) = 1.0, (c) = 2.0, (d) = 3.0, (e) = 4.0 and (f) = 5.0. $[Fe^{2+}]_0/(mg/L)$: ⬦ =1, ⬥ = 2, ⬦ = 3, ⬦ = 4, ⬥ = 5, ⬦ = 6, ⬥ = 7 and ⬥ = 8.

Table 3.16: The doses of KMnO$_4$ (measured as [Mn^{7+}] in percent of equivalent of [Fe^{2+}]$_o$) for varying coexisting [Mn^{2+}]$_o$ and [Fe^{2+}]$_o$ required to remove arsenic below 1 µg/L from initial 100 µg/L.

Coexisting [Mn^{2+}]$_o$ (mg/L)	Coexisting [Fe^{2+}]$_o$ (mg/L)							
	1	2	3	4	5	6	7	8
0.5	95	95	95	90	90	90	85	85
1.0	95	95	90	90	90	85	85	80
2.0	95	90	90	90	85	85	80	75
3.0	95	90	90	85	85	80	75	70
4.0	90	90	85	85	80	80	70	65
5.0	90	85	85	80	80	75	70	65

Table 3.17: The doses of NaHCO$_3$ (in mg/L) for varying coexisting [Mn^{2+}]$_o$ and [Fe^{2+}]$_o$ required to remove arsenic below 1 µg/L from initial 100 µg/L.

Coexisting [Mn^{2+}]$_o$ (mg/L)	Coexisting [Fe^{2+}]$_o$ mg/L							
	1	2	3	4	5	6	7	8
0.5	134	126	119	112	108	99	95	90
1.0	133	126	119	111	106	99	95	89
2.0	132	125	118	111	106	99	94	89
3.0	131	124	118	110	105	98	94	88
4.0	131	124	117	110	104	98	93	88
5.0	130	123	114	108	104	96	93	87

The coagulates formed by coexisting iron (Fe^{2+}) on oxidation and by externally added $FeCl_3$ are mainly iron oxides namely goethite (FeOOH), ferrihydrite ($5Fe_2O_3 \cdot 9H_2O$) and ferric hydroxide, $Fe(OH)_3$ formed depending upon the pH [273]. In the neutral pH of about 7.3 in the presence of $NaHCO_3$, the coexisting iron Fe^{2+} and externally added $FeCl_3$ forms coagulates predominantly goethite (FeOOH) [218] which adsorbs $H_2AsO_4^-$ and $HAsO_4^{2-}$ ions.

3.2.1.2. Optimization of the doses:

The results obtained from initial OCOP experiments presented in **Figure 3.11** were analysed by RSM using CCD and quadratic model to optimize the doses of $NaHCO_3$, $KMnO_4$ and $FeCl_3$ required for removal of arsenic, iron and manganese from groundwater to less than 1 µg/L, 0.03 mg/L and 0.009 mg/L, respectively [248].

The experimental CCD designs for the model with two independent parameters, namely, A and B, each of which has two coded levels as -1 and +1 for low and high concentrations/values, respectively. Levels of independent variables selected for the RSM analysis (low and high) of $[Fe^{2+}]_0$ are 1 mg/L and 8 mg/L; and that of $[Mn^{2+}]_0$ are 0.5 mg/L and 5.0 mg/L, respectively. The experimental data points used for optimization of required dose of $NaHCO_3$, $KMnO_4$, and $FeCl_3$ are included in **Table 3.18**. 3D Plot (a), (b) and (c) of **Figure 3.12** for doses of $KMnO_4$, $NaHCO_3$ and $FeCl_3$ respectively, was prepared using; **Equations (3.8)-(3.10)**, respectively, in terms of coded factors:

$$Y = 86.80 - 10.04 \times A - 6.46 \times B - 3.75 (A \times B) - 4.83 \times A^2 + 0.56 \times B^2 \qquad (3.8)$$

$$Y = 105.99 - 21.86 \times A - 1.69 \times B + 0.75(A \times B) + 4.57 \times A^2 - 0.013 \times B^2 \qquad (3.9)$$

$$Y = 4.14 - 3.45 \times A + 0.12 \times B + 1.250 \times 10^{-3}(A \times B) + 0.70 \times A^2 - 0.63 \times B^2 \qquad (3.10)$$

Where, the factors A and B represent $[Fe^{2+}]_0$ and $[Mn^{2+}]_0$ in **Equations (3.8)–(3.10).**

Table 3.18: The design of CCD for the dose of $KMnO_4$ (as $[Mn^{7+}]$ in percentage equivalent of $[Fe^{2+}]_o$), $[NaHCO_3]$ in mg/L and $FeCl_3$ (as $[Fe^{3+}]$ in mg/L) were taken as response, separately. All concentrations are in mg/L except for $[Mn^{7+}]$, which is in percentage equivalent of $[Fe^{2+}]_o$.

| Run	(a) $[Mn^{7+}]$ as response		(b) $[NaHCO_3]$ as response		(c) $[Fe^{3+}]$ as Response	
	Factor A $[Fe^{2+}]_o$	Factor B $[Mn^{2+}]_o$	Factor A $[Fe^{2+}]_o$	Factor B $[Mn^{2+}]_o$	Factor A $[Fe^{2+}]_o$	Factor B $[Mn^{2+}]_o$
1	4.50	2.75	4.50	2.75	4.50	4.00
2	4.50	1.00	4.50	5.93	8.00	0.50
3	1.00	5.00	4.00	0.50	4.70	2.75
4	1.00	2.75	4.50	2.75	4.50	2.75
5	8.00	5.00	8.00	0.50	1.00	0.50
6	9.45	2.75	9.45	2.75	4.50	4.89
7	4.50	2.75	1.00	5.00	12.57	2.75
8	4.50	2.75	8.00	5.00	4.50	2.75
9	4.50	2.75	1.00	2.75	4.50	2.75
10	4.50	2.75	4.50	2.75	4.50	2.75
11	4.50	5.93	4.50	0.50	1.00	5.00
12	8.00	0.50	4.50	2.75	8.00	5.00
13	1.00	0.50	4.50	2.75	4.50	2.75
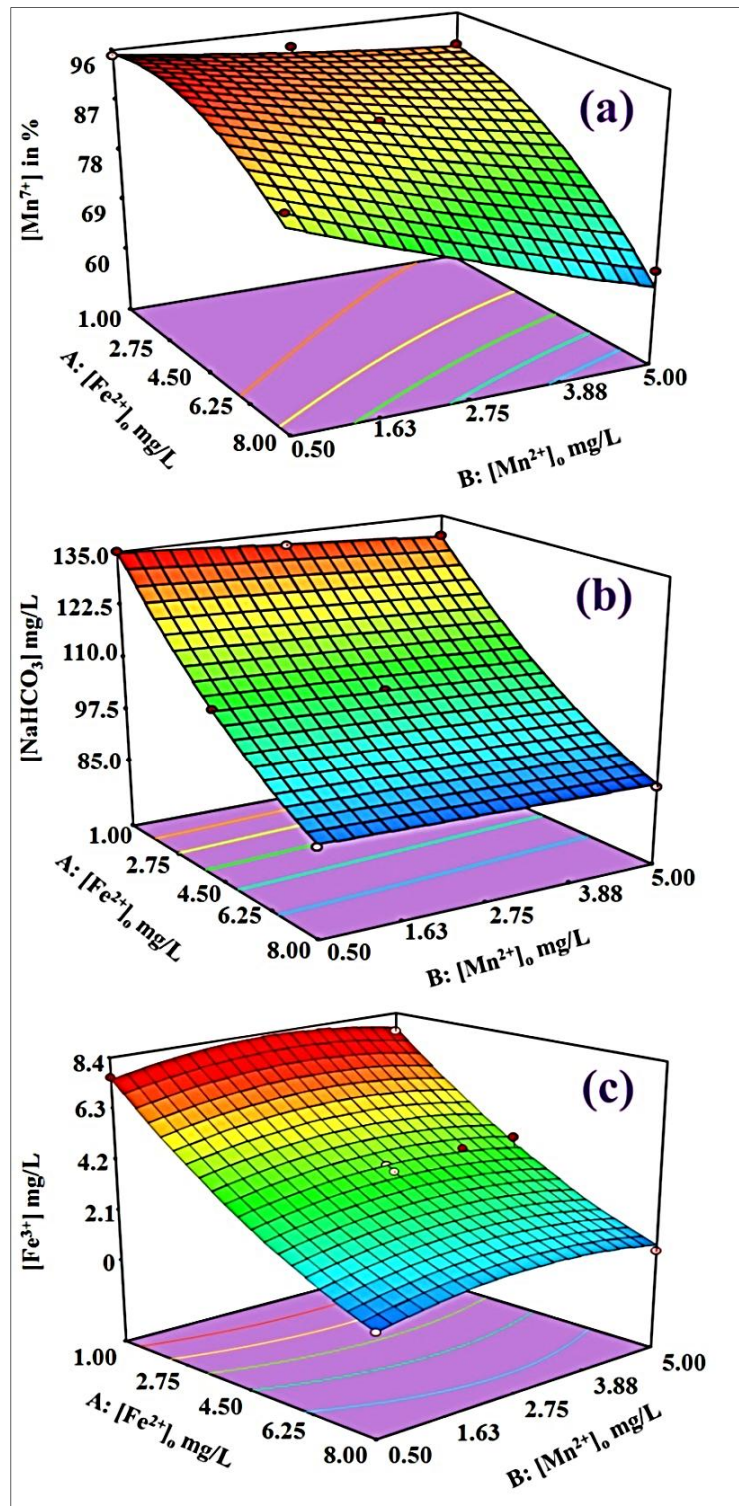
Figure 3.12: Plots of (a) 3D surface for required doses of KMnO$_4$ (measured as [Mn^{7+}] in percent of equivalent of [Fe^{2+}]$_o$) (b) 3D surface for required doses of NaHCO$_3$ in mg/L and (c) 3D surface for required doses of FeCl$_3$ (measured as [Fe^{3+}] in mg/L); with variation of [Fe^{2+}]$_o$ and [Mn^{2+}]$_o$ in mg/L for each plot to remove arsenic below 1 μg/L.

3.2.1.2.1. Validation of the model:

Validation of model of 3D plots of **Figure 3.12** is verified from diagnostics case studies. The normal probability plots of the residuals and the plots of the predicted versus actual response for surface roughness are shown in **Figure 3.13** obtained from diagnostics case studies [274]. A check on the plots in **Figure 3.13**; plot 1(a), 2(a) and 3(a) of **Figure 3.13** reveals that the residuals fall on a straight line implying that the errors are distributed normally. Moreover, the plots 1(b), 2(b) and 3(b) of **Figure 3.13** show that the predicted versus actual responses fall in the straight line signifying a well fitted model. According to this diagnostics case study of the model selected for the optimization of doses of $KMnO_4$, $NaHCO_3$ and $FeCl_3$ was found to be valid and reliable.

Confirmation of the fitting of the quadratic model of the 3D plots of **Figure 3.12** prepared by the CCD is given by Fisher's F-test. In this test, a p-value of less than 0.0500 is the indication of significant terms. For quadratic model of the 3D plots represented by plots (a), (b) and (c) of **Figure 3.12**, the p-value was found to be 0.0046, <0.0001 and <0.0001, respectively. So, the selected model was found to be fitted and suggested for analysis of varience (ANOVA). According to the ANOVA analysis, the model F-values of plot (a), (b) and (c) of **Figure 3.12** was found to be 58.57, 2142.30, and 285.34, respectively, indicating a significant model. The p-values less than 0.0500 indicate the models to be significant. ANOVA analysis for plot (a), (b) and (c) of **Figure 3.12** shows a highly reliable value of R^2, adjusted-R^2 and predicted-R^2 for quadratic model. All the Adequate Precisions of our models are found to be greater than 4 and therefore these models can be used to navigate the present design space. Sum of squares (SS), mean square (MS), F-value and P-value of the model and model terms of the 3D plots are presented in **Table 3.19** and R^2, adjusted R^2 and predicted R^2 values are presented in **Table 3.20**.
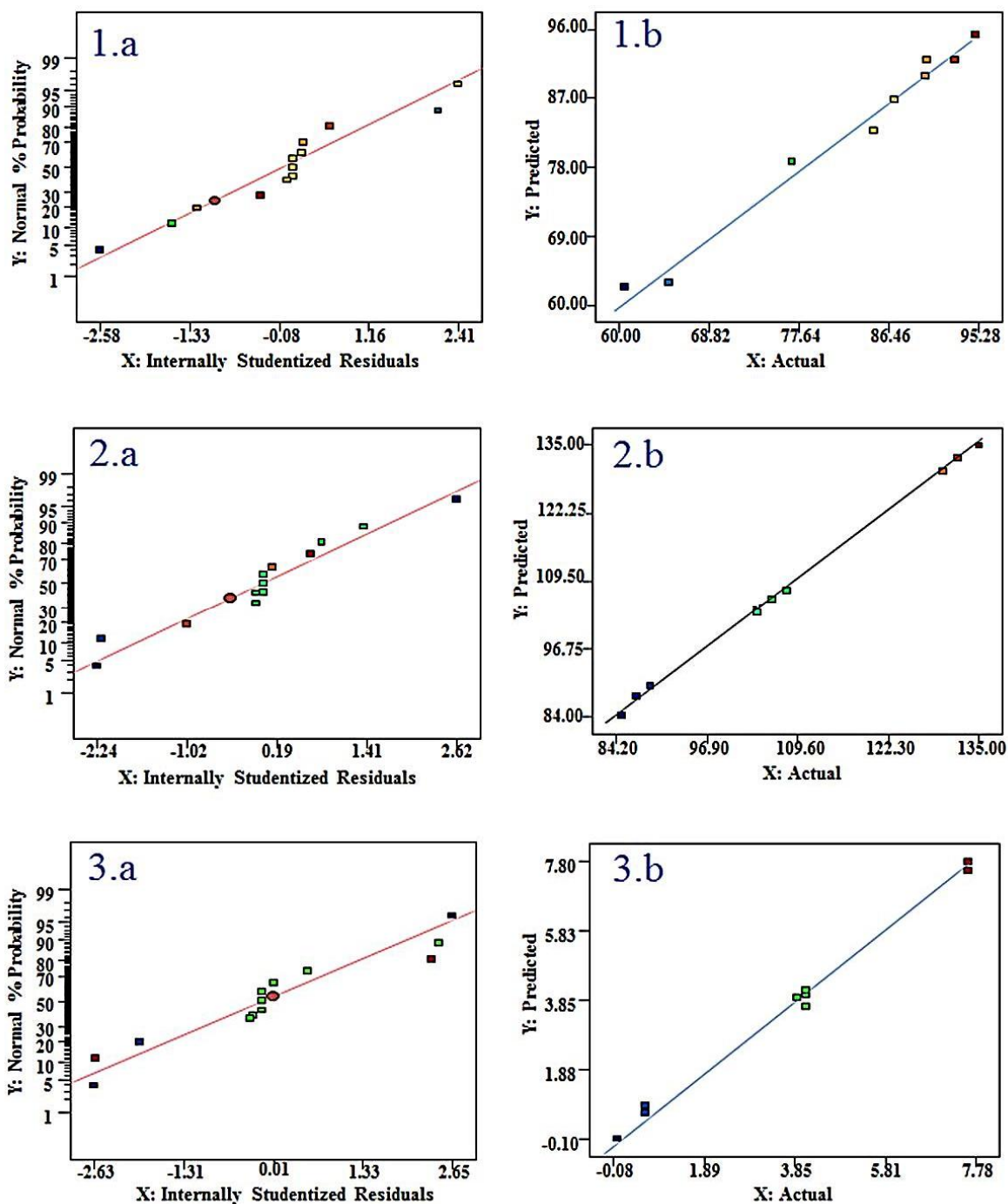
Figure 3.13: 1(a), 2(a), 3(a): Plot of internally studentized residuals vs. normal % probability of the model selected for optimization of $KMnO_4$, $NaHCO_3$ and $FeCl_3$ respectively. 1(b), 2(b), 3(b): Plot of predicted vs. actual, of the model selected for optimization of dose of $KMnO_4$, $NaHCO_3$ and $FeCl_3$, respectively.

Table 3.19: ANOVA results of Sum of squares (SS), Mean square (MS), F-value and P value of the model and model terms.

Figure 3.12 Plot (a)	SS	MS	F-value	P-value	Significance
Model	1275.21	255.04	58.57	< 0.0001	√
A	651.00	651.00	149.50	< 0.0001	√
B	237.39	237.39	54.52	0.0002	√
A×B	56.25	56.25	12.92	0.0088	√
A^2	111.19	111.19	25.53	0.0015	√
B^2	1.36	1.36	0.31	0.5932	×
Figure 3.12 Plot (b)					
Model	3152.71	630.54	2142.30	<0.0001	√
A	3094.68	3094.68	10514.35	<0.0001	√
B	18.40	18.40	62.51	<0.0001	√
A×B	2.25	2.25	7.64	0.0279	√
A^2	100.71	100.71	342.17	0.0001	√
B^2	8.563×10^{-4}	8.563×10^{-4}	2.909×10^{-3}	0.9585	×
Figure 3.12 Plot (c)					
Model	64.13	12.83	285.34	< 0.0001	√
A	49.01	49.01	1090.45	< 0.0001	√
B	0.065	0.065	1.44	0.2685	×
A×B	6.250×10^{-6}	6.250×10^{-6}	1.391×10^{-4}	0.9909	×
A^2	6.02	6.02	133.92	< 0.0001	√
B^2	1.01	1.01	22.42	0.0021	√

Table 3.20: The R^2, adjusted R^2 and predicted R^2 values of the 3D plots obtained by analysis of variance (ANOVA) along with standard deviation (SD), mean, C.V.%, precision and adequate precision (AP).

Figure 3.12 Plots (a)	SD	2.09	R^2	0.9767
	Mean	83.85	Adjusted R^2	0.9600
	C.V.%	2.49	Predicted R^2	0.9456
	Precision	322.69	AP	23.277
Figure 3.12 plot (b)	SD	0.54	R^2	0.9993
	Mean	107.69	Adjusted R^2	0.9989
	C.V.%	0.50	Predicted R^2	0.9941
	Precision	18.73	AP	137.395
Figure 3.12 plot (c)	SD	0.21	R^2	0.9951
	Mean	3.78	Adjusted R^2	0.9916
	C.V.%	5.62	Predicted R^2	0.8600
	Precision	64.88	AP	54.554

3.2.1.2.2. Findings from the RSM experiment:

By RSM analysis of the data of batch experiment we have prepared 3D plots using CCD design with fitted model as shown in **Figure 3.12**. From RSM analysis of this 3D plots (**Figure 3.12**) the required doses of $KMnO_4$ (as $[Mn^{7+}]$ in percentage equivalent (% eq) of $[Fe^{2+}]_o$), $NaHCO_3$ in mg/L and $FeCl_3$ (as $[Fe^{3+}]$ in mg/L) for different concentration of coexisting $[Fe^{2+}]_o$ and $[Mn^{2+}]_o$ were obtained to remove As, Fe and Mn from initial

concentration to below 1 µg/L, 0.03 mg/L and 0.009 mg/L respectively [248]. **Table 3.21** represents optimized doses of KMnO$_4$ (as [Mn^{7+}] in % equivalent of [Fe^{2+}]$_o$), NaHCO$_3$ (mg/L) and FeCl$_3$ (as [Fe^{3+}] mg/L) predicted by point prediction method. A comparison of the **Table 3.21** with **Table 3.16** and **Table 3.17**, shows that the doses of KMnO$_4$, NaHCO$_3$ and FeCl$_3$ predicted by RSM analysis shows good correlation with the experimentally found doses of KMnO$_4$, NaHCO$_3$ and FeCl$_3$ for removal of arsenic, iron and manganese to less than 1 µg/L, 0.03 mg/L, and 0.009 mg/L respectively. Therefore, our optimization of the required doses of KMnO$_4$, NaHCO$_3$ and FeCl$_3$ with respect [Fe^{2+}]$_o$ and [Mn^{2+}]$_o$ is good enough and is also capable of predicting the exact required doses for improved removal of arsenic in presence of coexisting Fe^{2+} and Mn^{2+} ions.

3.2.2. Field trial:

The doses of KMnO$_4$, NaHCO$_3$ and FeCl$_3$ used for the field trial are determined by the RSM analysis for various coexisting iron and manganese concentrations are presented in **Figure 3.14**. It is seen from **Figure 3.14** that the dose of FeCl$_3$ decreases with increase in [Fe^{2+}]$_o$ up to 8.607 mg/L as Fe beyond which, there is no need of externally added FeCl$_3$. However, required dose of KMnO$_4$ increases slightly with increase in [Fe^{2+}]$_o$ in the whole range as expected. With increase in [Fe^{2+}]$_o$ required dose of NaHCO$_3$ also decreases slightly because with increase in [Fe^{2+}]$_o$ required addition of FeCl$_{3,}$ a Lewis acid, decreases requiring more NaHCO$_3$ to raise the pH to 7.3 (±0.1).

Table 3.21: Optimized doses of KMnO$_4$ (as [Mn^{7+}] in percentage equivalent (% eq) of [Fe^{2+}]$_o$), NaHCO$_3$ in mg/L and FeCl$_3$ (as [Fe^{3+}] in mg/L) for different concentration of coexisting [Fe^{2+}]$_o$ and [Mn^{2+}]$_o$ obtained from RSM.

| Plot (a) of Figure 3.12			Plot (b) of Figure 3.12			Plot (c) of Figure 3.12		
Variables		Result	Variables		Result	Variables		Result
[Fe^{2+}]$_o$ mg/L	[Mn^{2+}]$_o$ mg/L	[Mn^{7+}] % eq	[Fe^{2+}]$_o$ mg/L	[Mn^{2+}]$_o$ mg/L	[NaHCO$_3$] mg/L	[Fe^{2+}]$_o$ mg/L	[Mn^{2+}]$_o$ mg/L	[Fe^{3+}] mg/L
2.23	1.56	93.57	5.21	0.85	103.05	2.87	4.04	5.76
6.15	3.07	79.80	6.94	4.36	92.12	7.78	0.59	0.82
7.61	4.80	65.60	6.06	4.95	95.81	4.95	4.34	3.47
1.62	0.59	95.54	1.13	2.35	131.71	7.14	1.28	1.58
2.23	4.10	89.07	3.85	3.04	109.98	1.24	1.09	7.53
3.33	4.92	85.13	2.15	0.95	124.44	4.70	3.14	3.94
3.71	1.95	90.88	2.03	1.33	125.11	2.57	3.50	6.22
7.47	4.20	68.82	2.84	2.86	117.32	3.84	2.71	4.81
6.15	2.96	80.26	6.81	1.47	94.24	5.57	3.93	3.03
7.07	4.59	69.65	6.11	3.63	96.38	5.19	1.57	3.25
6.09	1.26	86.87	1.88	4.64	123.02	4.06	1.68	4.38
6.90	4.90	69.50	6.62	0.54	95.63	5.81	3.76	2.87
5.85	4.54	76.61	2.14	2.39	123.14	2.19	1.64	6.51
6.40	1.16	86.20	7.06	1.79	92.93	2.74	1.55	5.80
5.16	1.20	89.94	1.33	1.83	130.50	3.37	3.72	5.25
3.64	3.45	87.30	5.70	0.57	100.42	3.82	4.86	4.78
2.29	3.04	90.68	7.55	4.87	89.40	6.48	3.65	1.96
2.10	3.36	90.39	5.03	1.12	103.94	4.75	3.73	3.83
5.52	0.84	90.27	3.23	3.58	113.80	2.94	2.79	5.82
6.88	2.18	78.80	6.76	1.94	94.22	3.53	4.52	4.85
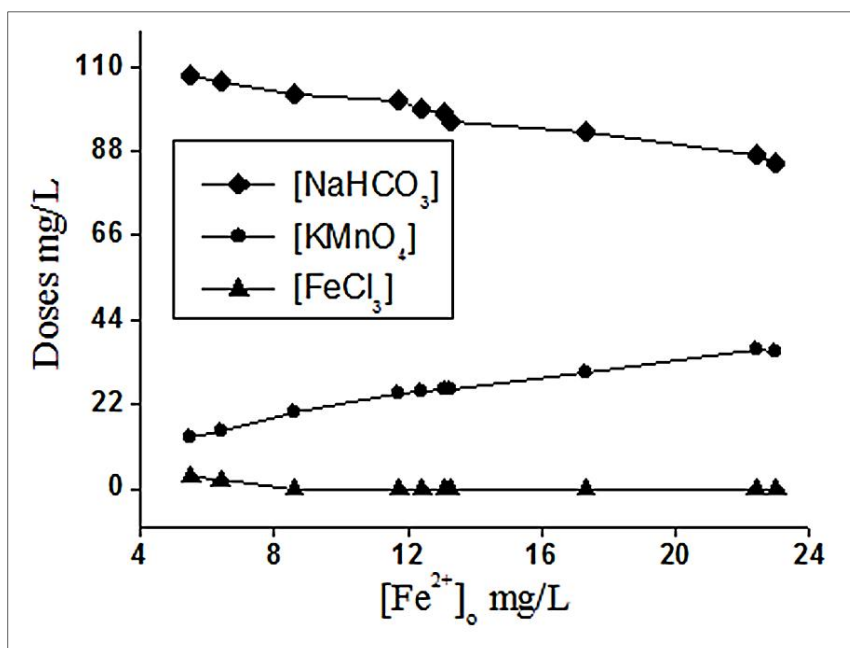
Figure 3.14: Plots of optimized doses of $NaHCO_3$, $KMnO_4$ and $FeCl_3$ for field trial of our experiment for different coexisting iron and manganese concentration.

The field trial showed very good removal of arsenic, iron and manganese as shown in **Figure 3.15**. Arsenic was removed from initial concentrations in the range of 91—25 μg/L to less than 1 μg/L presented in plot (a) of **Figure 3.15**. The removal of arsenic by the present modification of the OCOP method to such a low level is important in view of the WHO advice to remove arsenic to as low level as possible though it recommends a guideline value of 10 μg/L for drinking water as groundwater with levels as low as 0.17 μg/L can cause arsenicosis if consumed over a long period of time [55].

In **Figure 3.15**, plot (b) and plot (c) show that Fe^{2+} and Mn^{2+} ions were removed from initial concentrations in the range of 23–2 mg/L to less than 0.03 mg/L and of 0.5-1.9 mg/L to less than 0.009 mg/L, respectively. Thus, the present method simultaneously lowers the concentrations of As, Fe and Mn from contaminated groundwater to levels about ten times lower than the respective guideline values of 10 μg/L, 0.3 mg/L and 0.1 mg/L prescribed by the WHO.
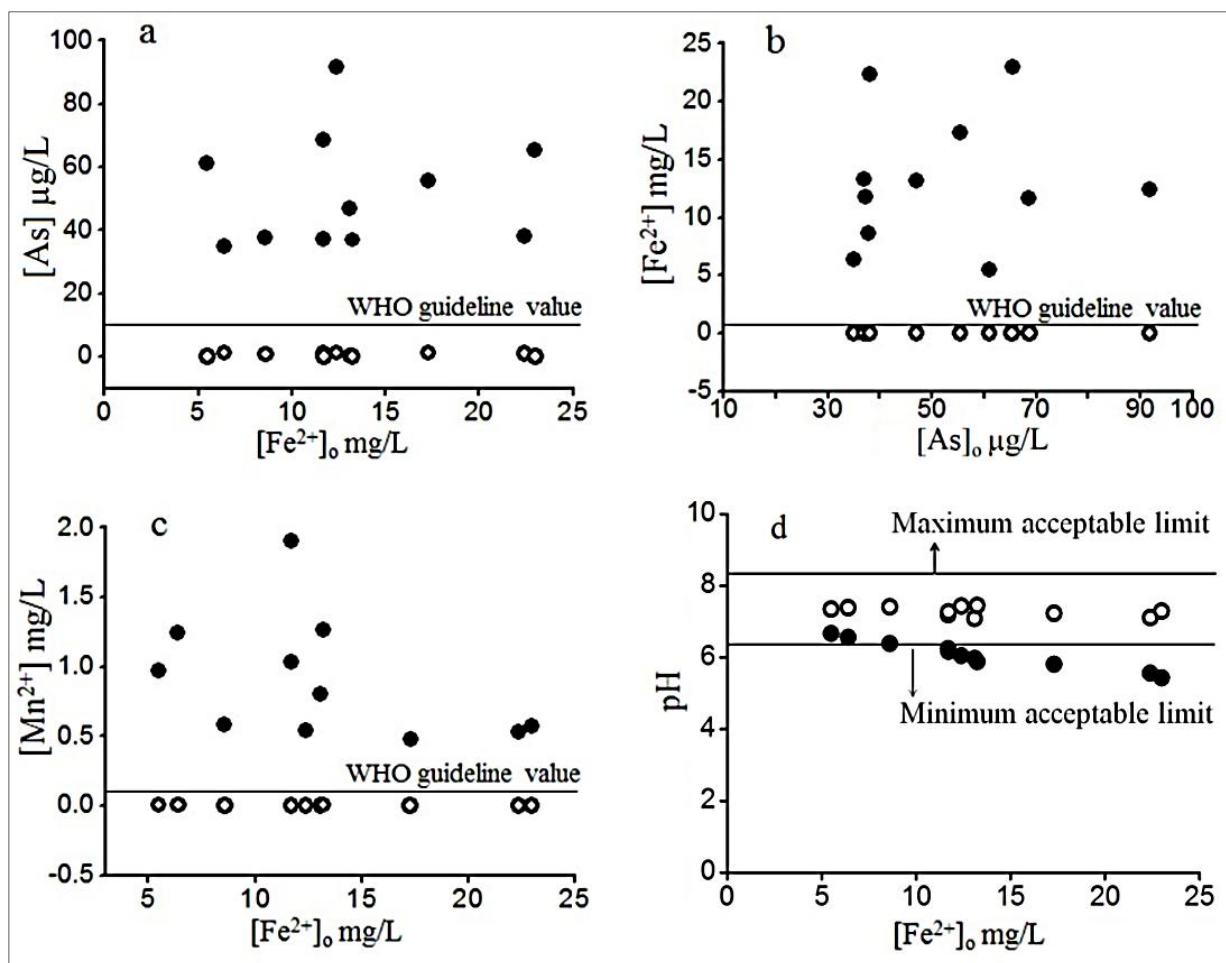
Figure 3.15: (a) Plot of concentration of total arsenic before and after the traetment, (b) plot of concentration of manganese before and after treatment, (c) plot of concentration of iron before and after the treatment, (d) plot of pH of the water smples before and after the treatment. Symbol: ● = before, ○ = after.

3.2.3. Suitability of the method:

The results of > 99% As^{3+} removal of the present study have been found to be far better than the previously reported results of < 30% As^{3+} removal by simple coagulation with ferric or aluminium salts [220, 275]. The results of the present method are also better than the reported 85-95% As^{3+} removal by coagulation with $FeCl_3$ after pre-oxidation of As^{3+} with $KMnO_4$ [276]. Plot (d) of **Figure 3.15** shows that final pH of the treated water samples are also found to be in the middle of the acceptable range 7.0–7.5 for drinking. The other relevant water quality parameters of the water before and after treatment have been found to be well within the respective WHO guideline values presented in **Table 3.22**.

An estimation of the cost of treatment; based on the current Indian retail price of NaHCO$_3$, KMnO$_4$ and FeCl$_3$; the cost of the present method has been found to be 0.326 USD per m^3 for simultaneous removal of As, Fe and Mn. This cost is slightly lower than the cost of removing As and Fe simultaneously by the earlier present modified OCOP method, modified earlier to utilize the coexisting iron in coagulation, which has been estimated to be 0.332 USD per m^3 based on the current prices. The slightly lower cost of the present method than the earlier modification can be attributed to the contribution of MnO$_2$ in As removal in the present method. The users showed good response and expressed their satisfaction with the simplicity of the method and the results.

Table 3.22: Major water quality parameters of the groundwater and synthetic water before and after the treatment by our present modified OCOP method

Water quality parameters*	WHO guideline Value	Groundwater	
		Before treatment	After treatment
Chloride (Cl$^-$)	250	6.7	9.89
Nitrate (NO$_3^-$)	50	<1.0	<1.0
Fluoride (F$^-$)	1.5	0.32	0.21
Sulphate (SO$_4^{2-}$)	500	7.8	7.5
Phosphate as P (PO$_4^{2-}$)	ns**	<0.003	<0.003
Sodium (Na$^+$)	Ns	5.63	13.4
Potassium (K$^+$)	Ns	10.9	8.7
Calcium (Ca^{2+})	75	0.88	0.80
Magnesium (Mg^{2+})	Ns	2.11	1.34
Silica (SiO$_2$)	Ns	4.37	2.78
Dissolved oxygen (DO)	Ns	81.4	76.6
Dissolved solids	600	132	171

*All parameters are in mg/L except DO, which is in percent, **Not specified
(Average % of error for triplicate experiment = 1.08%)

3.3. Evaluation of performance of different oxidizing agents in OCOP*:

This section presents the results of a study on performance of various oxidising agents in the OCOP.

3.3.1. Arsenic removal experiment:

In this work a set of OCOP experiments were performed in 1 L plastic mugs using tap water separately with varying quantities of oxidants, viz., $KMnO_4$, Fenton's reagent, NaOCl and H_2O_2 with fixed doses of 200 µg/L initial As^{3+} and 100 mg/L initial $NaHCO_3$ and 25 mg/L of $FeCl_3$. The dose of $KMnO_4$ was varied from 0.2 mg/L to 2 mg/L at an interval of 0.2 [277]. The doses of the other oxidants were also taken in equivalent of the dose of $KMnO_4$. After dosing, water was allowed to stay for 2 h and then the supernatant treated water was filtered with Whatman 42 filter paper for analysis. The effect of pH, temperature, and initial arsenic concentration on the best oxidant was also examined. Langmuir, Freundlich, and Temkin adsorption isotherm study was done with the best oxidant among the selected four oxidants to determine the adsorption capacity of coagulant formed from the oxidant.

3.3.2. Observation:

Figure 3.16 shows the plots of remaining total arsenic concentration from initial arsenic concentration ($[As^{3+}]_o$) of 200 µg/L after removal by OCOP method using $KMnO_4$, Fenton's reagent, NaOCl and H_2O_2 as the oxidizing agents. It is interesting to note that the removal of arsenic with Fenton's reagent and $KMnO_4$ were much better than that with NaOCl and H_2O_2. However, $KMnO_4$ has been found to be the best oxidizing agent, for removing As^{3+} by OCOP among all four oxidizing agents used, which closely followed by Fenton's reagent [277]. The results of removal of As^{3+} with $KMnO_4$ and Fenton's reagent are similar to that reported earlier with $KMnO_4$ [30, 218]. It may be noted here that the arsenic concentration decreased from 200 µg/L to 27-28 µg/L even without addition of any oxidant which may be attributed to aerial oxidation of As^{3+} to As^{5+} and adsorption As^{5+} by goethite coagulates obtained from addition of $FeCl_3$. While the plots of remaining arsenic *vs.* dose of the oxidant were found to be somewhat linear in cases of NaOCl and H_2O_2, rapid initial decreases in remaining arsenic were observed in the cases of Fenton's reagent and $KMnO_4$.

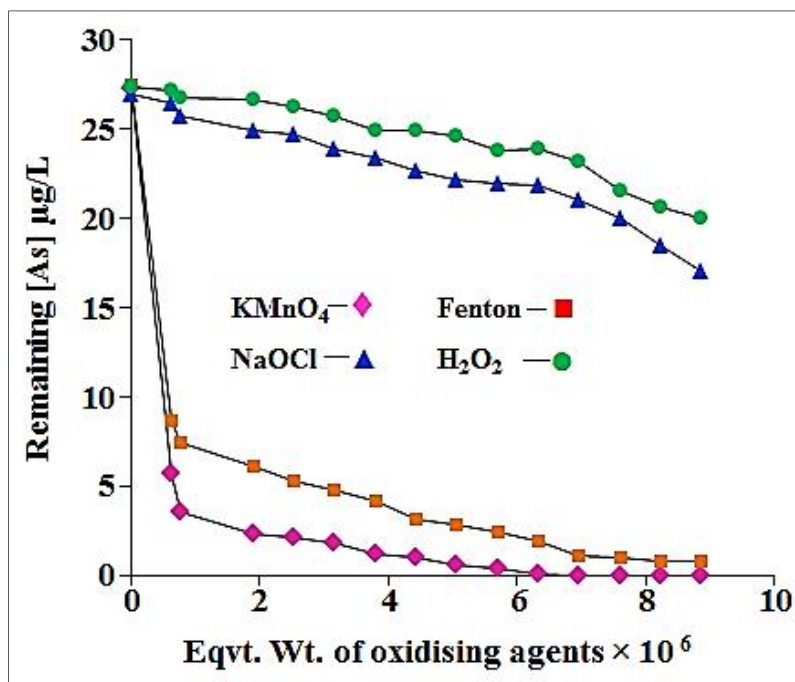*A paper on this work is published in *J. Water. Chem. Tech.* (2019)

Figure 3.16: Plot of remaining concentration of total arsenic from initial arsenite concentration of 200µg/L after removal of arsenic by OCOP with varying concentrations of the oxidising agents.

Figure 3.16 also shows that for the dose 0.2 mg/L of $KMnO_4$, which is equal to an equivalent concentration of 0.632×10^{-6}, the As removal efficiency has been found to be 97.12%. It may be noted that the doses of $FeCl_3$ and $NaHCO_3$ were fixed at 25 mg/L and 100 mg/L, respectively. The doses of Fenton's reagent, NaOCl and H_2O_2 equivalent (0.632×10^{-6}) to that of 0.2 mg/L of $KMnO_4$ are 1.19 mg/L, 0.14 mg/L and 0.14 mg/L, respectively. With the equivalent dose of 0.632×10^{-6}, the As removal efficiency of Fenton's reagent, NaOCl and H_2O_2 have been found to be 95.6%, 86.7%, and 86.4%, respectively. The As removal efficiency was found to increase remarkably on increasing the oxidant dose. On increasing the dose, removal of As reaches 100% at a dose of 2 mg/L (Equivalent concentration of 6.327×10^{-6}) of $KMnO_4$. The equivalent dose of 6.327×10^{-6} of Fenton's reagent (11.9 mg/L), NaOCl (1.41 mg/L) and H_2O_2 (1.41 mg/L) could remove As to 98.8%, 89.0% and 88.0%, respectively. Among the chosen oxidants, the performance of $KMnO_4$ in removal of As has been found to be the best followed by Fenton's reagent. Highest removal efficiency is found in case of $KMnO_4$ because during oxidation As^{3+} to As^{5+} $KMnO_4$ itself reduces to MnO_2 which also helps in removal of arsenic by adsorbing on its surface [97]. The oxidation of As^{3+} to As^{5+} by $KMnO_4$ in OCOP can be represented as:

$$3H_3AsO_3 + 2KMnO_4 + 4OH^- \rightarrow 3HAsO_4^{2-} + 2MnO_2 + 5H_2O + 2K^+ \qquad (3.11)$$
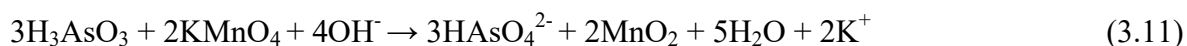
The observed better arsenic removal efficiencies of Fenton's reagent compared to that of NaOCl and H_2O_2, in equivalent concentration of $KMnO_4$, may be attributed to adsorption of arsenate ions on insoluble iron oxides formed from $FeCl_3$ and oxidation of ferrous iron of Fenton's reagent [278]. The better performance of $KMnO_4$ than Fenton's reagent also indicate a greater contribution of manganese dioxide, MnO_2 to arsenate adsorption than that by ferric oxides produced from Fenton's reagent. In addition to a slightly better performance of $KMnO_4$ in arsenic removal than Fenton's reagent the former may be preferred due to its ease of handling.

3.3.2.1. Effect of pH:

Figure 3.17 shows removal of arsenic by OCOP at different pH. The observed rapid and linear increase in the removal of arsenic in the acidic conditions up to about pH 4.5 may be attributed to first dissociation (pK_{a1} = 4.503) [80] of H_3AsO_4 through reaction (3.12) occurring in this pH range.

$$H_3AsO_4 = H_2AsO_4^- + H^+ \qquad (3.12)$$

Similarly, the second somewhat rapid and linear increase in the removal of arsenic in the pH range from about 6.5 to 7.5 may be attributed to the second dissociation (pK_{a2} = 7.09) [279] of H_3AsO_4 through reaction (3.13).

$$H_2AsO_4^- = HAsO_4^{2-} + H^+ \qquad (3.13)$$

Interestingly, the pH of the treated water after OCOP remains at approximately 7.3 (±0.1), at which $KMnO_4$ removes arsenic below ND.
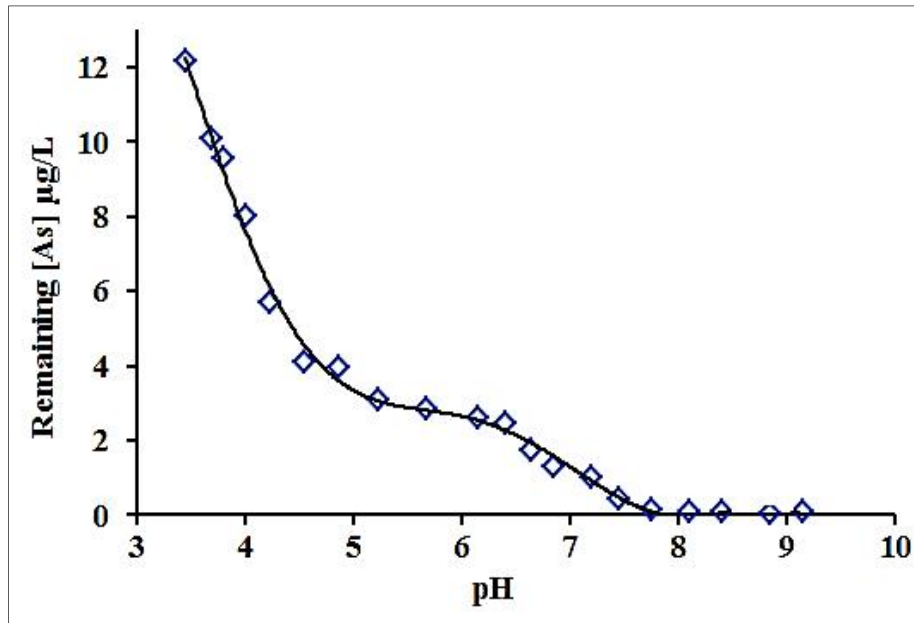
Figure 3.17: Arsenic removal at varying pH using KMnO$_4$ as oxidant in OCOP. Initial [As^{3+}]$_o$ was 200 µg/L.
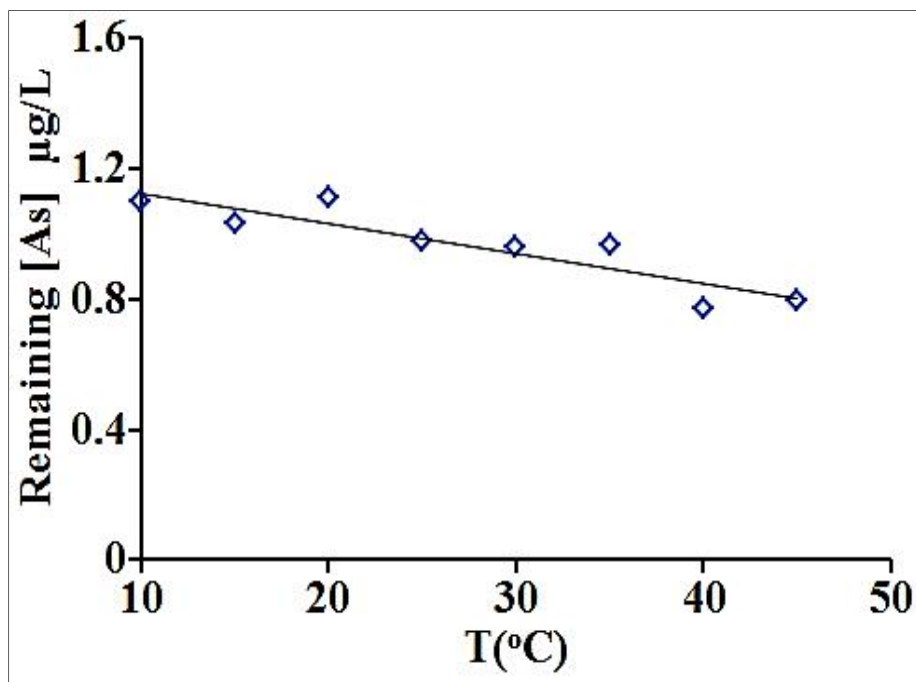

Figure 3.18: Remaining total arsenic concentration, [As] after the OCOP experiments at varying temperatures.

3.3.2.1. Effect of temperature:

The results of OCOP experiments with initial arsenic concentration of 200 µg/L and fixed dose of $NaHCO_3$, $KMnO_4$ and $FeCl_3$ at varying temperatures from 10^oC to 45^oC are shown in **Figure 3.18.** One can see from the figure that arsenic removal by OCOP method linearly increases with temperature and is highly effective between 10^oC to 45^oC indicating applicability of the method within this temperature range.

3.3.2.1. Effect of initial arsenic concentration:

OCOP experiments were performed with varying $[As^{3+}]_o$ from 100 µg/L to 500 µg/L in an interval of 50 µg/L as there is no reports on the applicability of the method with respect to $[As^{3+}]_o$. **Figure 3.19** shows the removal of arsenic with respect to varying $[As^{3+}]_o$ after the OCOP treatment with fixed dose of $NaHCO_3$, $KMnO_4$ and $FeCl_3$ as 100 mg/L, 2 mg/L and 25 mg/L, respectively. For all $[As^{3+}]_o$ in the range, the remaining arsenic concentration is found below the WHO guideline value for drinking water, *i.e.,* 10 µg/L. The concentration of remaining arsenic has been found to be a polynomial function of fourth order of initial arsenic concentration. The removal of arsenic at higher $[As^{3+}]_o$, however, can be further improved by adjusting the doses [248].
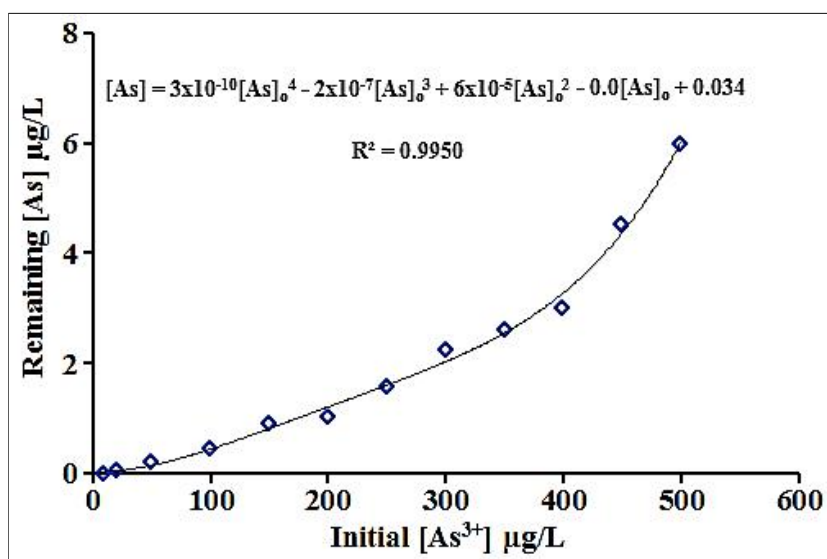

$$[As] = 3 \times 10^{-10}[As]_o^4 - 2 \times 10^{-7}[As]_o^3 + 6 \times 10^{-5}[As]_o^2 - 0.0[As]_o + 0.034$$

$$R^2 = 0.9950$$

Figure 3.19: Plots of remaining arsenic concentration after the treatment by OCOP method for different initial $[As^{3+}]$ with fixed dose of $NaHCO_3$, $KMnO_4$ and $FeCl_3$ as 100 mg/L, 2 mg/L and 25 mg/L, respectively.

3.3.2.1. Adsorption isotherms:

For experiments on adsorption of arsenic on the coagulates and precipitates during OCOP were conducted with varying $[As^{3+}]_0$ between 100 and 500 µg/L and fixed doses of 2 mg/L $KMnO_4$ and 25 mg/L $FeCl_3$. Here, the fixed initial dose of the adsorbent is taken as the sum of the quantities in mg/L of MnO_2 and FeOOH produced at the chosen doses of $KMnO_4$ and $FeCl_3$ assuming the adsorbent to consist of precipitates of MnO_2 and FeOOH [218]. The total quantity of the so-formed adsorbent has been calculated as 14.8 mg/L with a ratio of MnO_2: FeOOH as 1.2:13.7. The equilibration time was 2 h. Adsorption data were fitted to Freundlich, Langmuir and Temkin adsorption isotherms [261]. The Linear form of Freundlich isotherm can be represented by **Equation 3.14**:

$$\ln(Q_e) = \ln(K_F) + 1/n \ln(C_e) \tag{3.14}$$

where, Q_e, C_e, K_F and n are the amount of arsenic adsorbed at equilibrium (mg/g), the arsenite concentration at equilibrium (mg/L), the Freundlich adsorption capacity (mg/g) and adsorption intensity, respectively. The values of K_F and n were determined from the intercept and slope of the linear plot of $\ln(Q_e)$ *vs.* $\ln(C_e)$. From Freundlich isotherm presented in **Figure 3.20(a)**, we have found for the present case that the value R^2, K_F and n to be 0.9754, 537 and 1.58 respectively.

The Langmuir isotherm can be written as **Equation 3.15**:

$$C_e/q_e = C_e/Q_o + 1/bQ_o \tag{3.15}$$

where, Q_o and b are the adsorption capacity (mg/g) based on Langmuir isotherm and the Langmuir isotherm constant (L/mg) related to the affinity of the binding sites, respectively. The Q_o and b values were calculated from slope and intercept of the plot of C_e/Q_e *vs.* C_e. From Langmuir isotherm shown in **Figure 3.20(b)**, it has been found that the value of R^2, Q_o and b is 0.9750, 29.0, and 2.90×10^5, respectively.
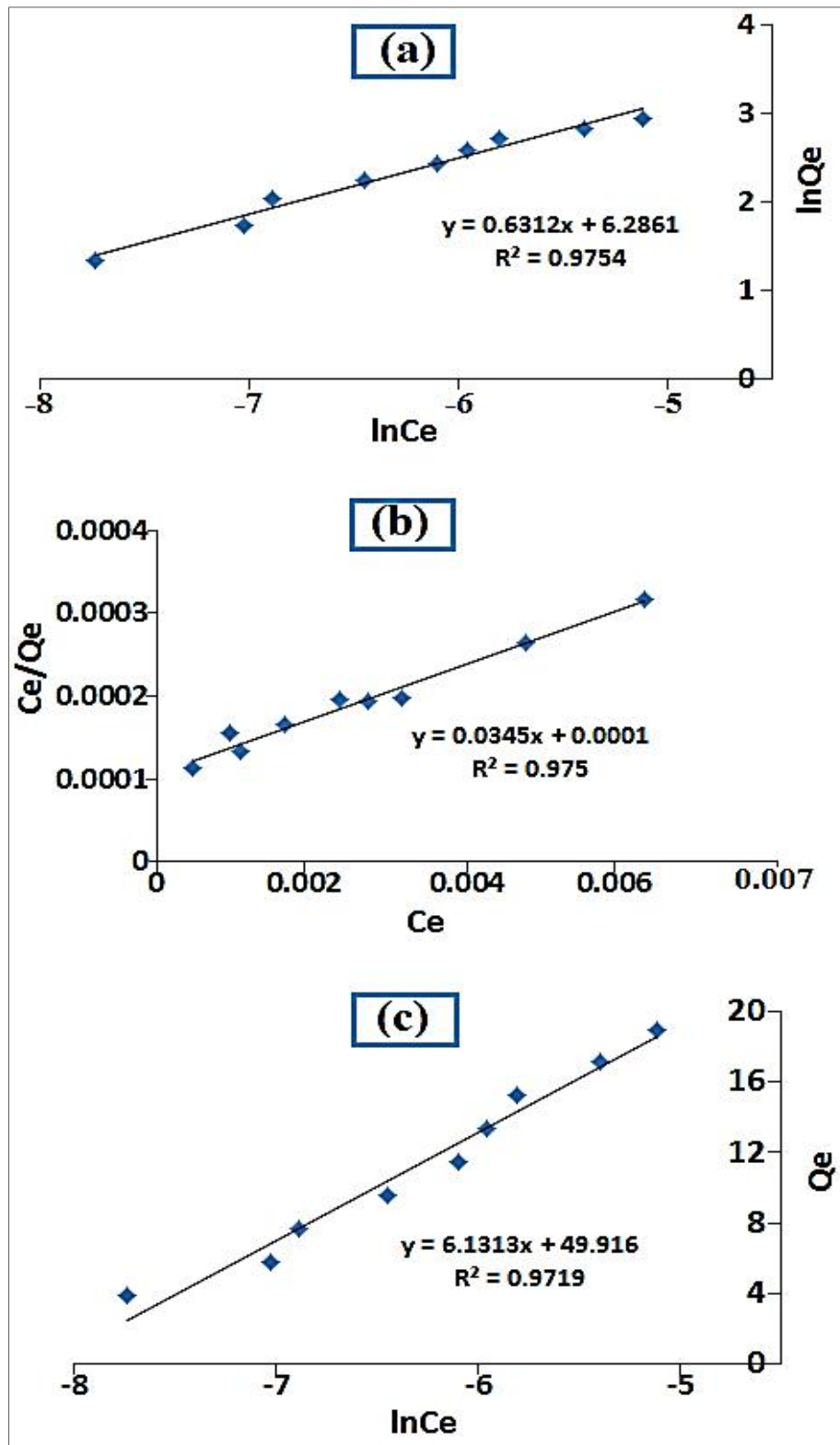
Figure 3.20: Plot of Freundlich (a), Langmuir (b) and Temkin (c) isotherm of the adsorbent formed during OCOP treatment.

The Temkin isotherm equation can be written as **Equation 3.16**.

$$Q_e = B_T \ln(A_T) + BT \ln(C_e) \tag{3.16}$$

where, A_T (L/g) is the binding constant that represents the maximum binding energy and B_T = (RT)/b is the Temkin constant related to heat of sorption. These constants have been evaluated from the plots of Qe *vs*. ln(Ce). The values of R^2, B_T and A_T for the for the Temkin isotherm presented in **Figure 3.20(c)** have been found to be 0.9719, 6.13and 3433 respectively.

Interestingly, Freundlich, Langmuir and Temkin plots have shown almost equal R^2 values, indicating similar moderate fitting of the adsorption data to all three models of adsorption which is an unusual observation. We attribute this observation to the fact that the arsenic adsorption by adsorbent mixture of MnO_2 and FeOOH, formed in the present case, starts right from the nucleation of the solid entities of MnO_2 and FeOOH, which continues during the growth of the precipitate of MnO_2 and coagulates of FeOOH or a mixture of them until completion of the process. Thus, arsenic is bound not only on the solid surfaces but also within the solids and is neither exactly a multilayer nor a monolayer adsorption. In other words, arsenic is chemisorbed on heterogeneous surface and inside the precipitates MnO_2 and FeOOH formed by $KMnO_4$ and $FeCl_3$. However, the observed high values of Temkin constants A_T and B_T suggests adsorption to be the mechanism of binding of arsenic rather than ion-exchange.

3.4. Removal of some metals: Cd, Pb, Ni, Cr, Cu and Co by OCOP*:

The results of our study on removal of some heavy metals in addition to arsenic, iron and manganese have been presented in this section.

3.4.1. Laboratory Experiment:

A series of OCOP experiments with fixed doses of $NaHCO_3$, $FeCl_3$ and $KMnO_4$ was carried out in 1 L mug for this study. A set of experiments with variation of initial concentration of the heavy metals from 2 mg/L to 10 mg/L with a fixed treatment time of 2 h is verified to see the capacity of removal of heavy metals by OCOP. After that the treated water was allowed to coagulate and settle down. The supernatant clear water was then filtered through Whatman 42 filter paper.

Another set of experiment with mug containing 1 L synthetic contaminated water with a fixed 5 mg/L initial concentrations of each of Cu^{2+}, Cr^{6+}, Ni^{2+}, Cd^{2+}, Pb^{2+}, and Co^{2+}, respectively, in separate mugs. The filtrate was collected after varying residence time from 1 to 4h. All the filtrates obtained after the experiments were analysed by AAS to determine remaining concentrations of the heavy metals.

3.4.2. Observations:

3.4.2.1. Removal of the metals with variation of initial concentrations:

Figure 3.21 shows removal of the hazardous heavy metal, namely, Cd, Pb, Ni, Cr, Co, and Co from contaminated groundwater with variation of initial concentration of the metal ions from 2 mg/L to 10 mg/L [284]. Interestingly, all six metal ions have been found to be removed considerably after the OCOP treatment. The percentage of removal of all heavy metals increased with decrease in the initial concentration of the heavy metals. The removal of the metals from equal initial concentration of 2 mg/L was found to increase in the order Cd (79.0%) << Co (94.8%) < Ni (94.4%) << Cu (98.0%) < Cr (98.3%) < Pb (99.5%) [284].

---

*A paper based on this work has been published in *J. Water Process. Eng.*, 31:1-9, 2019.

3.4.2.1.1. Comparison of the result with explanation:

The removal of Pb has been found to be competitive with 99.3% reported with electrocoagulation [117]. The observed 98.3% removal of total Cr is far better than 91% reported with ferric chloride alone and 95% reported with ferric chloride and polymer [108]. 98% Cu removal by the present method is also far better than reported 74.8% removal with CNTs and 83.3% removal with CNTs/AC [182]. In OCOP method, the mild alkaline pH provided by $NaHCO_3$ may favour precipitation of the heavy metals [118]. The present results are also better than reported 80% removal of Cd, Pb, Zn, Ni, Cu and Cr^{3+} from an initial concentration of 2 mg/L by limestone, with a final pH of 8.5, which is in the higher side of the acceptable range of pH for drinking water [110]. Thus, the OCOP method, with a removal efficiency of 94.4-99.5% and with a final pH of 7.3, removes Cd, Pb, Ni, Cr, Cu and Co also very well from drinking water.

The observed low removal of Cd may be attributed to weaker binding/adsorption to oxygen of FeOOH coagulates or MnO_2 precipitates formed during OCOP treatment due to its soft acidic nature [280]. On the other hand Cr, being a hard acid [280], is removed very well due to its strong binding FeOOH and MnO_2. Further evidences are required to explain the observed order of ease of removal of the other heavy metal ions. The initial concentration ranges of the heavy metals used in this study were above the concentration range in which they occur in groundwater due to limitation of the atomic absorption spectrophotometer in detecting the metal ions in microgram per litre level. However, the percentage removals of the metal ions were found to increase gradually with decrease in initial concentrations of the metal ions.

3.4.2.1.2. Remarks on the results:

Pb and Cd are reported to be present up to 0.215 mg/L and 0.110 mg/L, respectively, in groundwater. Considering the percentage removals of Pb and Cd to be at least equal to that observed at initial concentration of 2 mg/L, the estimated remaining concentrations of the metal ions after OCOP treatment are 0.001 mg/L and 0.024 mg/L against their WHO guideline values of 0.01 mg/L and 0.003 mg/L, respectively. The heavy metal ions of Pb, Cr, Cu, Ni and Cd are estimated to be removed below their respective WHO guideline values from initial concentrations of at least 2 mg/L, 7.5 mg/L, 80 mg/L, 0.81 mg/L, and 0.014 mg/L, respectively.
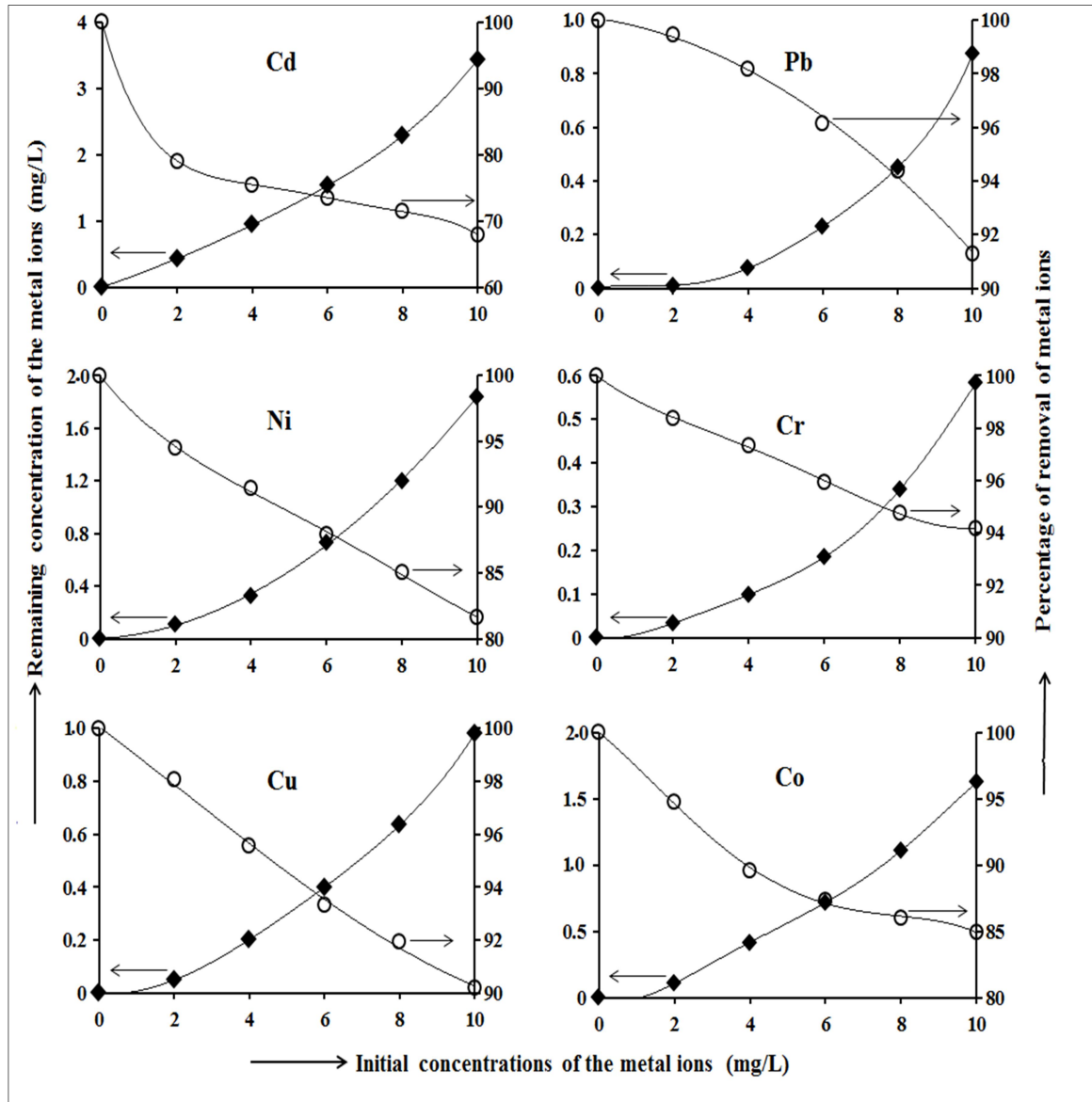
Figure 3.21: Plots of remaining concentrations of Cd, Pb, Ni, Cr, Cu, and Co in mg/L (primary Y-axis, closed diamond-♦) and % of removal (secondary Y-axis, open circle-○) against initial concentration in mg/L after OCOP treatment.

Literatures reveals that heavy metal concentration in natural groundwater is usually found below 2 mg/L [55,74–77, 281], and therefore the OCOP method, with 94.4-99.5% of removal, is highly efficient for removal of heavy metals from groundwater. Thus, OCOP is capable of removing Pb, Cr, Cu, Co and Ni to safe level from their respective ranges of concentrations in which they generally occur in groundwater except for Cd.

3.4.2.2. Removal of the metals with variation of resident time:

Figure 3.22 shows the results of removal of these heavy metals from initial concentration of 5 mg/L by OCOP method with variation of residence time up to 4 h. Removal was found to increase with increase in residence time. The removal levelled off above 3 h for Cd and Co which is the optimum residence time for most adsorption methods [282, 283] but continued to decrease up to 4 h in the case of Pb, Cr, Ni and Cu. This experiment indicates that more residence time is required for maximum removal of these heavy metal ions than that of 2 h, normally required for OCOP treatment for removal of arsenic and iron.

3.4.3. Analysis of the precipitate or coagulates obtained in the OCOP experiment:

3.4.3.1. Analysis by AAS:

For AAS analysis of the heavy metals present in the coagulates of OCOP, the solid obtained from the process was dissolved in aqua regia (mixture of nitric acid and hydrochloric acid, optimally in a molar ratio of 1:3). The volume of each solution was adjusted to 1 L with distilled water. **Figure 3.23** shows the plots of the concentrations of the heavy metals in the aqua regia extract of coagulates obtained after the removal experiment of heavy metals by OCOP at varying initial concentrations. The concentrations of the heavy metals in the extracts of the solid obtained in OCOP process have shown good correlation with the initial concentrations of the heavy metals.
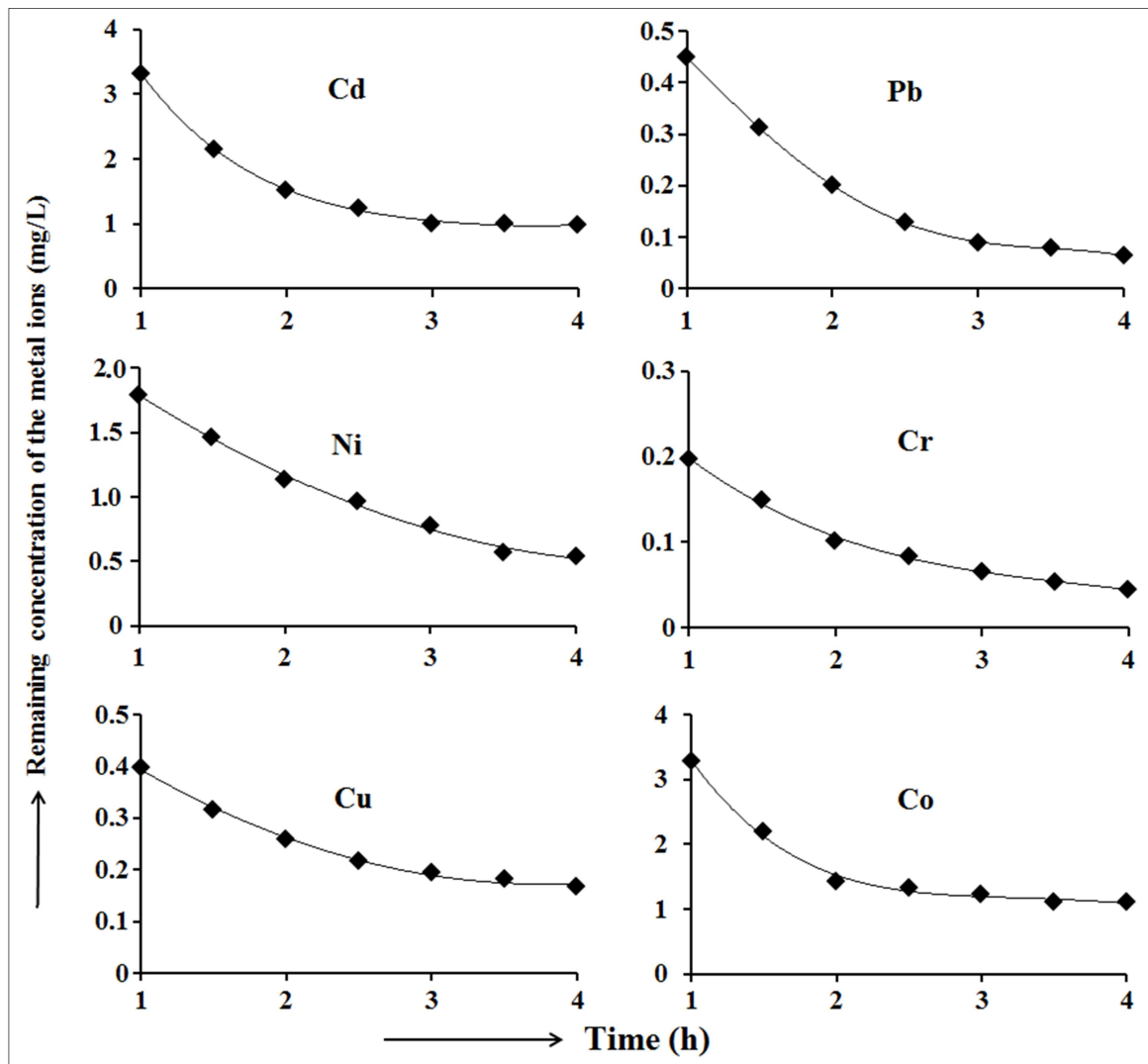
Figure 3.22: Plots of remaining concentrations of Cd, Pb, Ni, Cr, Cu, and Co in mg/L measured after varying residence time in hour at initial concentration of 5 mg/L in OCOP treatment.
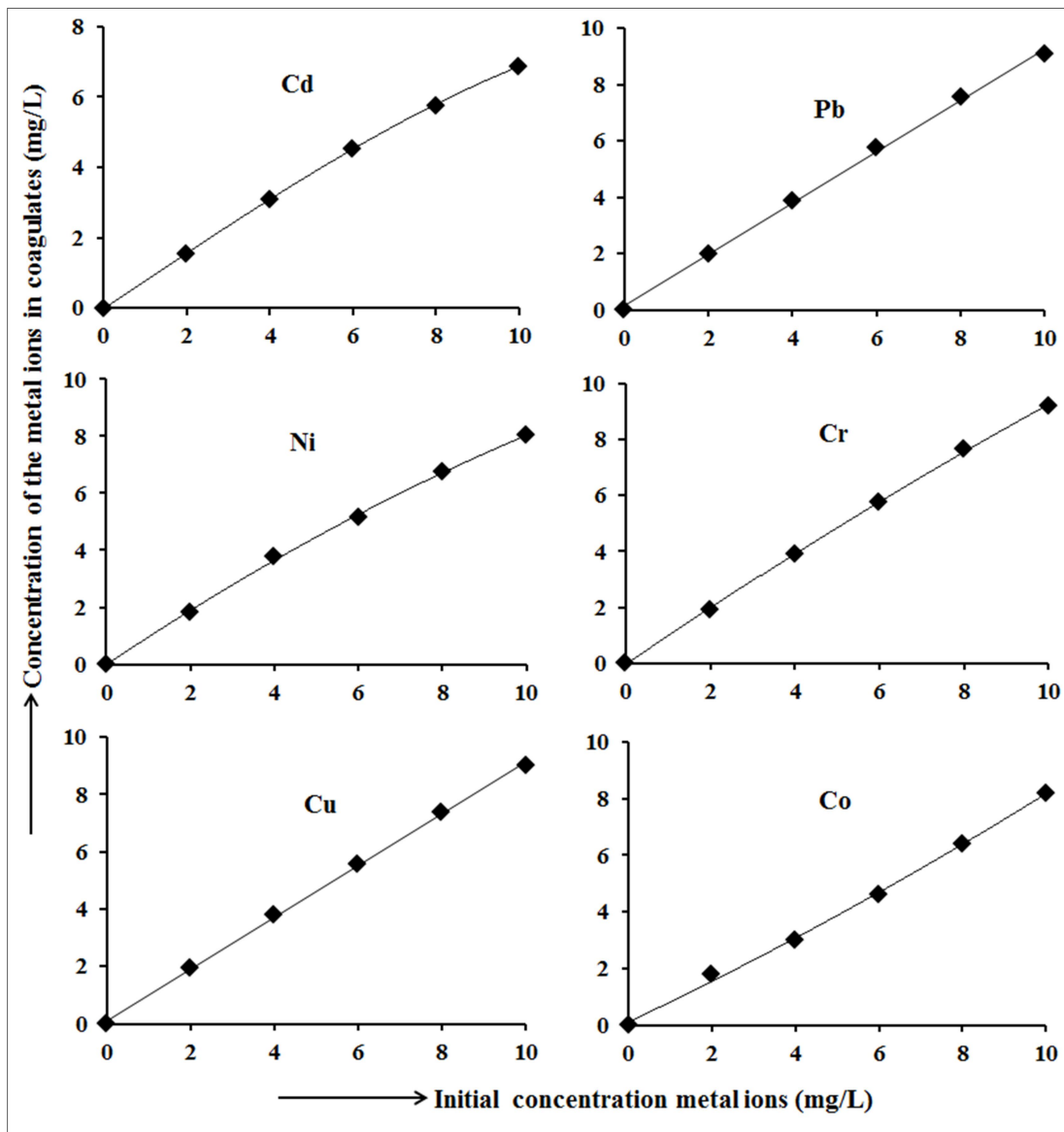
Figure 3.23: Plots of concentration of the Cd, Pb, Ni, Cr, Cu, and Co against initial concentrations in mg/L found in the aqua-regia extract of coagulates obtained from the OCOP experiments.

Plot of sum of concentrations of the metal in filtrate and in the extract of coagulate against the initial concentrations of the metals have been shown in **Figure 3.24**. It is interesting to note that the sums of remaining concentration and the concentration observed in the extract were in good agreement with the corresponding initial

concentrations for the heavy metal ions within experimental error limits. The observed experimental error limits were 1.16, 1.14, 3.43, 0.91, 0.42, and 3.36 percent for Cd, Pb, Ni, Cr, Cu, and Co, respectively. This indicates a very little escaping of detection by AAS by any of the heavy metal.
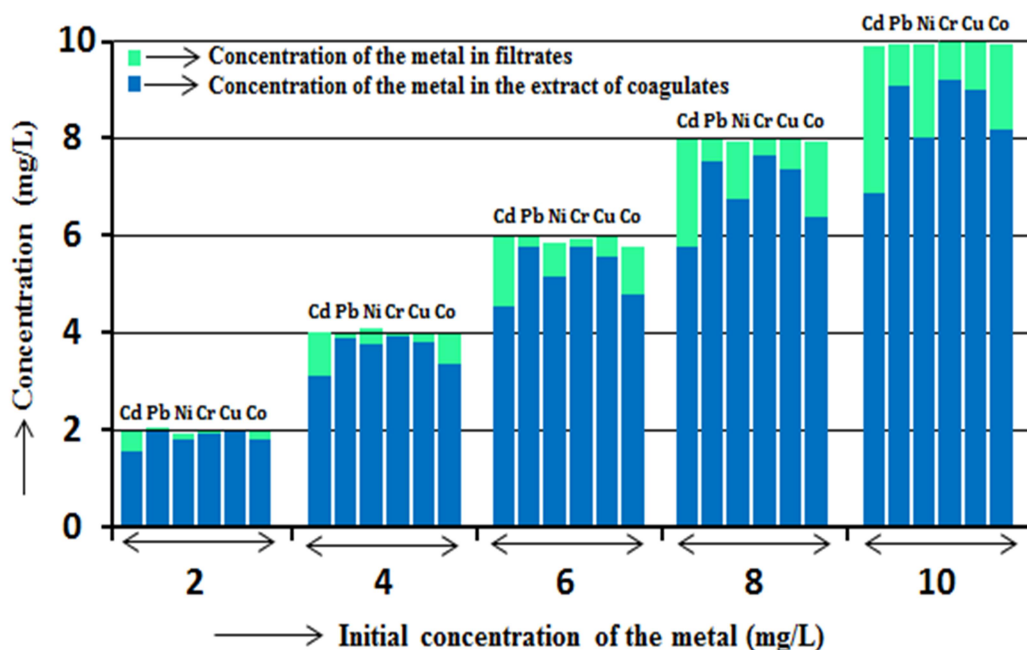

Figure 3.24: Plot of sum of concentrations of the metal in filtrate and in the extract of coagulate against the initial concentrations of Cd, Pb, Ni, Cr, Cu, and Co, respectively. Experimental error limits: Cd (1.16%), Pb (1.14%), Ni (3.34%), Cr (0.91%), Cu (0.91%), and Co (3.36%).

3.4.3.2. Analysis by EDX:

The EDX estimation of the heavy metals in the solid obtained from the OCOP experiment with performed separately for individual metal ions with initial concentration of the metal ions as 5 mg/L and residence time of 2 h are shown in **Figure 3.25**. The spectra obtained for each metal ion showed the presence of the respective elements. While the percentage composition with respect to weight of the Cd, Pb, Ni, Cr, Cu and Co in the precipitates or coagulates were 6.39, 21.82, 2.32, 2.13, 13.87 and 7.54 percent, respectively; the atomic percentage were 1.15, 2.33, 0.82, 0.70, 3.95 and 2.90 percent, respectively. The observed disagreement in atomic percentage may be attributed to difference in removal of the individual metal ions and inhomogeneous nature of the mixtures.
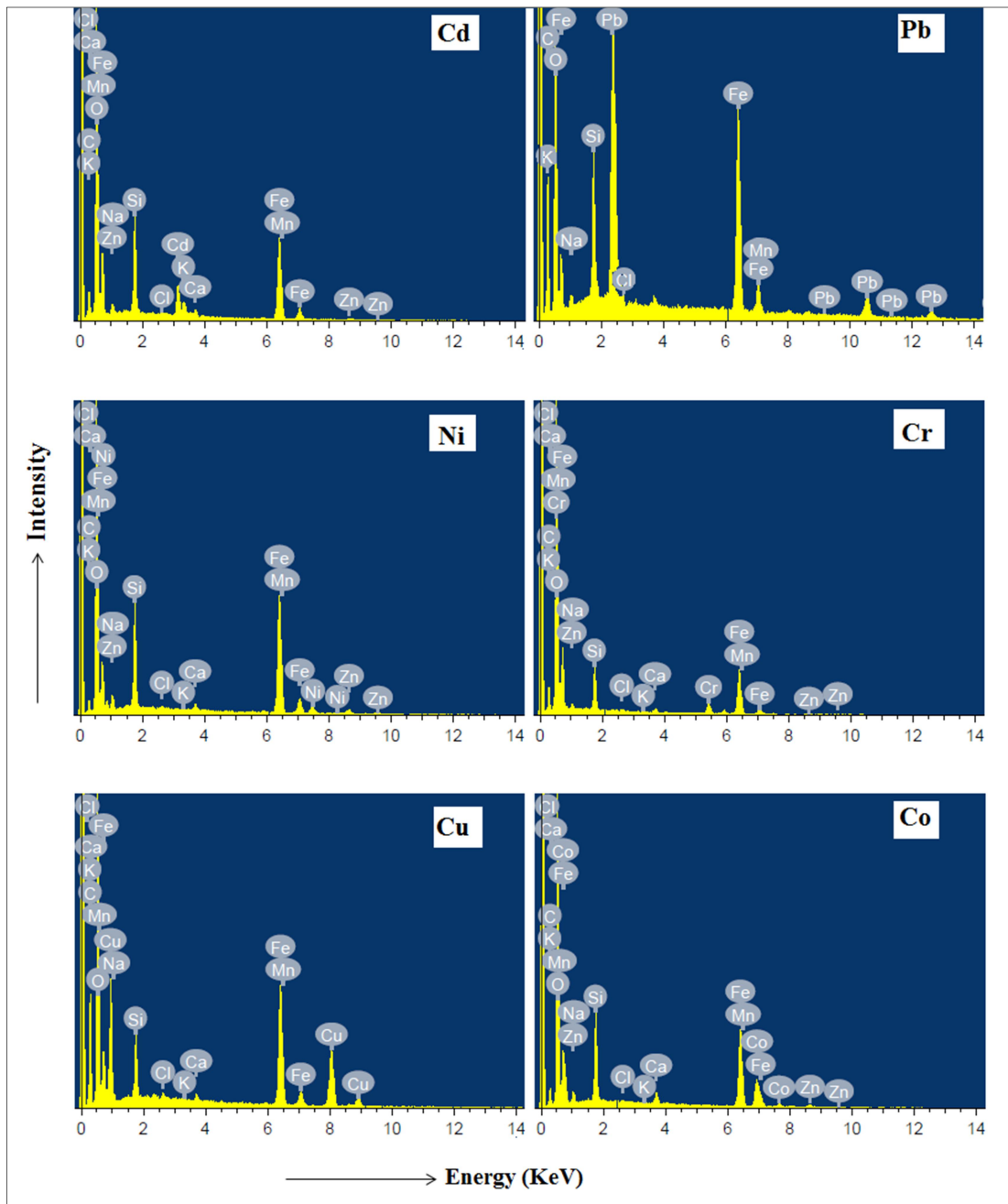
Figure 3.25: EDX spectra of the solids obtained after OCOP treatment for removal of Cd, Pb, Ni, Cr, Cu and Co with initial concentrations of 5 mg/L.

3.4.3.3. Analysis by XRD:

The XRD pattern of the solid coagulates of OCOP method in the absence of the heavy metals can be seen elsewhere [218]. While the XRD pattern of the solid obtained from OCOP treatment in the presence of Co (**Figure 3.26f**) showed a highly amorphous nature of the coagulated solid like that obtained in absence of any of the heavy metals, the XRD spectra of the solids obtained in the presence of Ni, Cr and Cu indicated formation of partially amorphous solids, and the XRD patterns of the solid formed in the presence of Cd and Pb indicated highly crystalline solids (**Figure 3.26a-e**).

The XRD spectra with the plane value (h k l) of the solid coagulates obtained in presence of the heavy metals with initial concentrations of 5 mg/L obtained during the present OCOP experiments are shown in **Figure 3.26**. The XRD of the solid obtained in the presence of Cd showed sharp peaks at 2θ=30.42 (1 0 3), 60.8 (2 1 5), and 63.07 (1 1 6) due to Mn_3O_4 complex (JCPDS No: 652776; 800382, 652776; and 800382, 651298, respectively), as can be seen in **Figure 3.26a**. Peaks observed at 2θ=36.49 (4 0 0), 43.8 (4 0 1), 49.89 (3 0 2), and 58.1 (5 2 1) were due to the presence of MnO_2 compound in the coagulates (JCPDS No: 721982; 651298; 721982, 651298; and 530633, respectively). The pattern at 2θ=40.17 (2 1 0), 48.06 (4 1 1) and 75.12 (2 0 2) confirms the existence of goethite, FeOOH (JCPDS No: 810464). Cadmium oxide, CdO_2 formation resembles with the XRD pattern at 2θ=65.69 (3 2 1) (JCPDS No: 781125) and complexes $Cd_{0.1}Mn_{0.9}O$ and $Cd_2Mn_3O_8$ also resembles with XRD pattern at 2θ=40.19 (2 1 0) (JCPDS No: 896000) and 61.56 (3 3 1) (JCPDS No: 721428), respectively.

The XRD spectra of the solid obtained in the presence of Pb (**Figure 3.26b**) shows peaks at 2θ=20.10 (1 1 0), 35.62 (1 1 0), 40.82 (1 1 3), 43.50 (1 1 4), 45.83 (1 3 3), 47.04 (2 1 3) and 49.04 (1 4 2) (JCPDS No: 897047; 898103, 898104, 897047; 898103, 897047; 898103, 897047; 897407; 897407; 897407; and 897407, respectively) as evidences of formation of iron oxide, Fe_2O_3 in the solid. XRD peaks at 2θ=34.65 (0 2 1) (JCPDS No: 810463) indicates presence of goethite, FeOOH. XRD peak at 2θ=29.12 (1 0 0), 36.19 (2 0 0), 62.67 (3 1 1) and 64.10 (2 0 1) (JCPDS No: 440872; 652873, 040686; 870663 and 440872, respectively) are the evidences for the elemental precipitation/co-precipitation of Pb with coagulates. XRD pattern at 2θ=56.40 (3 0 4) and 59.2 (5 2 1) (JCPDS No: 898912) reveals the formation of the compound Pb(Fe,Mn)12O19.

The XRD spectra obtained in the presence of Ni (**Figure 3.26c**) shows peaks at $2\theta=30.20$ (2 2 0) and 30.25 (2 2 0) (JCPDS No: 862267, 893080) indicative of formation of $NiFe_2O_4$ and NiO compound, respectively. XRD pattern at $2\theta=34.6$ (0 2 1) (JCPDS No: 810463) evidences the formation of FeOOH in the coagulates. **Figure 3.26d** represents the XRD pattern in the presence of Cr. The XRD peak at $2\theta=26.89$ (0 11 0) (JCPDS No: 361330) indicates formation of chromium oxide, Cr_3O_8 during the experiment. XRD pattern at $2\theta=35.62$ (1 1 0) (JCPDS No: 898103) is due to iron oxide Fe_2O_3. **Figure 3.26e** represents the XRD pattern of coagulates obtained in the presence of Cu. XRD peak at $2\theta=31.28$ (0 6 6) (JCPDS No: 752146, 791546 and 390246) is due to the formation of $Cu(FeO_2)$. XRD peak at $2\theta=35.22$ (1 1 1) (JCPDS No: 892530) evidences co-precipitation of the Cu ions with coagulates.

3.4.4. Mechanism of removal:

Co being very similar to iron gave amorphous solids like that containing iron alone produced in absence of any heavy metal. Presence of Ni, Cr and Cu in the water leads to formation of some crystalline compounds of $NiFe_2O_4$ and NiO, Cr_3O_8, and $Cu(FeO_2)$, respectively. The presence of Cd leads to formation of highly crystalline compounds of CdO_2, $Cd_{0.1}Mn_{0.9}O$ and $Cd_2Mn_3O_8$ in addition to facilitating formation of crystalline FeOOH, MnO_2 and Mn_3O_4. Similarly, the presence of Pb in the solid coagulates indicates formation of $Pb(Fe,Mn)_{12}O_{19}$ in addition to facilitating formation of crystalline Fe_2O_3 and FeOOH.

The XRD analysis complements the understanding of the order of ease of removal of the heavy metals in the OCOP treatment: Cd< <Co < Ni< <Cu < Cr < Pb. As mentioned earlier in Section 3.1, Cd^{2+} ion, being a soft acid [282] is least adsorbed onto FeOOH and MnO_2 and is removed mainly through precipitation of crystalline CdO_2, $Cd_{0.1}Mn_{0.9}O$, and $Cd_2Mn_3O_8$ resulting in least removal among the chosen heavy metals. Formation of CdO_2 may be possible due to the oxidation of Cd^{2+} to Cd^{4+} by addition $KMnO_4$ because $KMnO_4$ which is well known strong oxidizing agent. Formations of the complexes $Cd_{0.1}Mn_{0.9}O$ and $Cd_2Mn_3O_8$ are possible because in these complexes oxidation state of Cd is +2 and in water generally heavy metals precipitates as oxides and hydroxides [285, 286]. Co is removed only by adsorption onto amorphous FeOOH and MnO_2, and therefore removed much more than Cd but comparatively less than the other moderately hard acid metal ions.
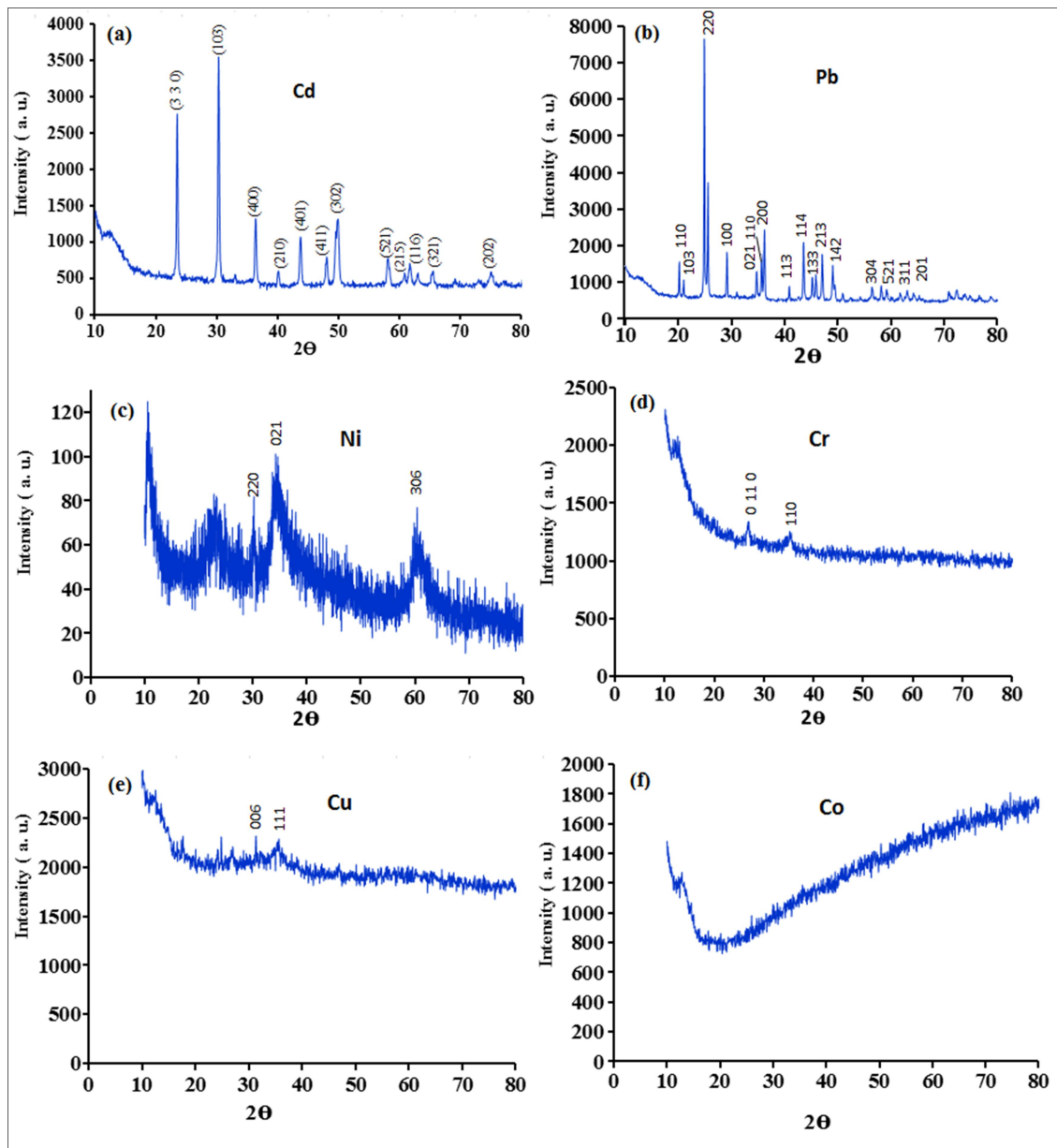
Figure 3.26: XRD patterns of the coagulates obtained when treated water contains initial concentration of (a) Cd, (b) Pb, (c) Ni, (d) Cr, (e) Cu, and (f) Co respectively.

Ni is removed better than Co due to formation of come crystalline $NiFe_2O_4$ and NiO in addition to adsorption. In water heavy metals like Ni^{2+} form hydroxide or oxide at higher pH [287]. The formation of $NiFe_2O_4$ may result from conversion of NiO due during heating and drying of the coagulates before analysis. This heating effect is also reported in several articles according to the following **Equation 3.17** [287, 288].

$$FeOOH + Ni(OH)_2 \rightarrow \alpha\text{-}Fe_2O_3 + Ni0 \rightarrow NiFe_2O_4. \tag{3.17}$$

The removal of Cu^{2+}, Pb^{2+}, and Cd^{2+} may also be facilitated by co-precipitations with the iron hydroxides or oxide such as FeOOH and Fe_2O_3 [289, 290]. Cu is probably adsorbed stronger than Co and Ni due to its smaller size. Cr is adsorbed very strongly due to its hard acidic nature as mentioned earlier. The highest removal of Pb may be attributed to co-precipitation along with precipitation of highly crystalline $Pb(Fe,Mn)_{12}O_{19}$ in addition to moderate adsorption as a moderately hard acid [280].